Electronic Supplementary Information (ESI)

# Understanding Structure-Activity Relations and Performance of Highly Active Novel ATRP Catalysts

Konstantin W. Kröckert,[a] Felix Garg,[a] Michel V. Heinz,[a] Justin Lange,[a] Patricia P. Simões,[a] Regina Schmidt,[a] Olga Bienemann,[b] Alexander Hoffmann[a] and Sonja Herres-Pawlis*[a]

## Table of Contents

Christallographic Data and Parameters ..... 2
Cyclic voltammogramms ..... 6
Polymerisation kinetics ..... 9
NMR-spectra ..... 15
UV/Vis spectra ..... 22
EPR-spectra ..... 24

[a] *Institut für Anorganische Chemie, RWTH Aachen University, Landoltweg 1a, 52074 Aachen (Germany). E-mail: sonja.herres-pawlis@ac.rwth-aachen.de*
[b] *Fakultät für Chemie und Chemische Biologie, Technische Universität Dortmund, Otto-Hahn-Str.6, 44227 Dortmund (Germany).*

## Christallographic Data and Parameters

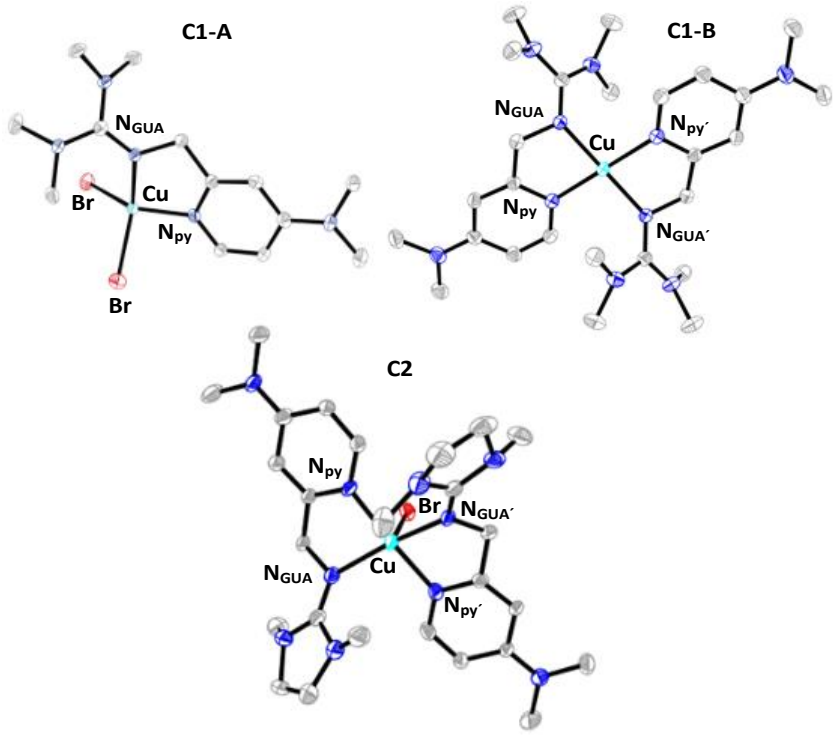


**Fig. S1** Molecular structure of the complex in crystals of [Cu(TMGm4NMe$_2$py)Br$_2$] (**C1-A**) and of the cationic complex units in crystals of [Cu(TMGm4NMe$_2$py)$_2$]Br$_2$ (**C1-B**) and [Cu(DMEGm4NMe$_2$py)$_2$Br]Br·C$_5$H$_{12}$ (**C2**)in the solid state (ellipsoids drawn at the 50% probability level). H atoms and solvent molecules are omitted for clarity.

**Table S1** Crystallographic data and parameters of the Cu(II) complexes [Cu(TMGm4NMe$_2$py)Br$_2$] (**C1-A**), [Cu(TMGm4NMe$_2$py)$_2$]Br$_2$ (**C1-B**), [Cu(DMEGm4NMe$_2$py)$_2$Br]Br·C$_5$H$_{12}$ (**C2**).

| Complex/Ligand | **C1-A** | **C1-B** | **C2** |
|---|---|---|---|
| Empirical formula | $C_{13}H_{23}Br_2CuN_5$ | $C_{26}H_{46}Br_2CuN_{10}$ | $C_{26}H_{42}Br_2CuN_{10}$ [+$C_5H_{12}$] |
| Formula mass [g mol$^{-1}$] | 472.72 | 722.09 | 718.05 |
| Crystal size [mm] | 0.15 x 0.14 x 0.12 | 0.35 x 0.30 x 0.24 | 0.18 x 0.17 x 0.04 |
| T [K] | 100(2) | 100 | 100(2) |
| Crystal system | Monoclinic | Triclinic | Monoclinic |
| Space group | $P2_1/n$ | $P$-1 | $P2_1/c$ |
| a [Å] | 8.7711(18) | 9.2630(19) | 12.868(3) |
| b [Å] | 19.273(4) | 9.5980(19) | 21.016(4) |
| c [Å] | 10.732(2) | 10.712(2) | 13.142(3) |
| α [°] | 90 | 77.80(3) | 90 |
| β [°] | 103.29(3) | 66.20(3) | 94.75(3) |
| γ [°] | 90 | 83.30(3) | 90 |
| V [Å$^3$] | 1765.6(7) | 851.2(4) | 3541.9(12) |
| Z | 4 | 1 | 4 |
| $\rho_{calcd.}$ [g cm$^{-3}$] | 1.778 | 1.409 | 1.347 |
| μ [mm$^{-1}$] | 5.764 | 3.020 | 2.903 |
| λ [Å] | 0.71073 | 0.71073 | 0.71073 |
| F(000) | 940 | 371 | 1468 |
| *hkl* range | -10/10, -23/23, -13/13 | -13/13, -14/14, -15/15 | -17/18, -30/29, -18/18 |
| Reflections collected | 21006 | 16399 | 51931 |
| Independent reflections | 3465 | 5899 | 10461 |
| $R_{int.}$ | 0.0279 | 0.0290 | 0.0781 |
| No. parameters | 196 | 200 | 360 |
| $R_1$ [I≥2$\sigma$(*I*)] | 0.0532 | 0.0757 | 0.0737 |
| $wR_2$ (all data) | 0.1221 | 0.2248 | 0.1757 |
| Goodness-of-fit | 1.196 | 1.125 | 1.035 |
| $\Delta\rho_{fin}$ max/min [eÅ$^{-3}$] | 2.028/-1.174 | 2.412/-1.835 | 1.124/-0.760 |

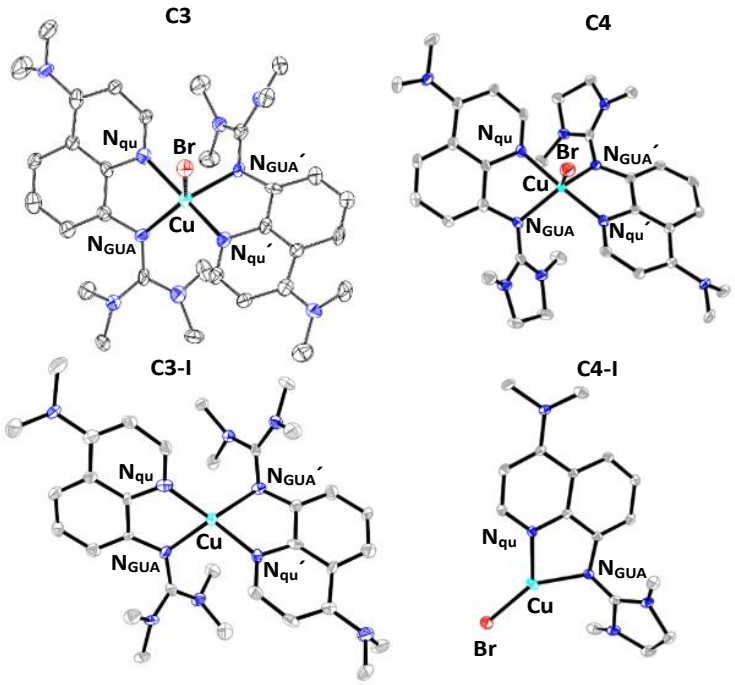


**Fig. S2** Molecular structure of the cationic complex units in crystals of [Cu(TMG4NMe$_2$qu)$_2$Br]Br·2 $C_4H_{10}O$ (**C3**), [Cu(TMG4NMe$_2$qu)$_2$]Br·THF·$CH_2Cl_2$ (**C3-I**), [Cu(DMEG4NMe$_2$qu)$_2$Br]Br·$CH_3CN$ (**C4**) and of the complex in crystals of [Cu(DMEG4NMe$_2$qu)Br] (**C4-I**) in the solid state (ellipsoids drawn at the 50% probability level). H atoms and solvent molecules are omitted for clarity.

**Table S2** Crystallographic data and parameters of the Cu(II) complexes [Cu(TMG4NMe$_2$qu)$_2$Br]Br·2 $C_4H_{10}O$ (**C3**) and [Cu(DMEG4NMe$_2$qu)$_2$Br]Br·$CH_3CN$ (**C4**) and of the Cu(I) complexes [Cu(TMG4NMe$_2$qu)$_2$]Br·THF·$CH_2Cl_2$ (**C3-I**) and [Cu(DMEG4NMe$_2$qu)Br] (**C4-I**).

| Complex | **C3** | **C3-I** | **C4** | **C4-I** |
|---|---|---|---|---|
| Empirical formula | $C_{32}H_{46}Br_2CuN_{10}$ [+ 2 $C_4H_{10}O$] | $C_{33}H_{48}BrCl_2CuN_{10}$ [+ $C_4H_8O$] | $C_{32}H_{42}Br_2CuN_{10}$ [+ $CH_3CN$] | $C_{16}H_{21}BrCuN_5$ |
| Formula mass [g mol$^{-1}$] | 794.15 | 799.16 | 790.11 | 426.83 |
| Crystal size [mm] | 0.62 x 0.16 x 0.15 | 0.18 x 0.16 x 0.14 | 0.28 x 0.16 x 0.10 | 0.14 x 0.11 x 0.06 |
| T [K] | 100(2) | 100(2) | 100(2) | 100(2) |
| Crystal system | Triclinic | Orthorhombic | Triclinic | Monoclinic |
| Space group | $P\bar{1}$ | $P2_12_12_1$ | $P\bar{1}$ | $P2_1/c$ |
| a [Å] | 11.581(2) | 11.531(2) | 11.840(2) | 14.212(3) |
| b [Å] | 13.967(3) | 14.073(3) | 12.829(3) | 8.3493(17) |
| c [Å] | 14.017(3) | 25.526(5) | 13.614(3) | 14.873(3) |
| α [°] | 72.17(3) | 90 | 64.90(3) | 90 |
| β [°] | 85.97(3) | 90 | 88.44(3) | 106.54(3) |
| γ [°] | 73.20(3) | 90 | 73.15(3) | 90 |
| V [Å$^3$] | 2065.8(9) | 4142.5(14) | 1781.3(8) | 1691.7(6) |
| Z | 2 | 4 | 2 | 4 |
| $\rho_{calcd.}$ [g cm$^{-3}$] | 1.277 | 1.281 | 1.473 | 1.676 |
| μ [mm$^{-1}$] | 2.495 | 1.655 | 2.893 | 3.659 |
| λ [Å] | 0.71073 | 0.71073 | 0.71073 | 0.71073 |
| F(000) | 814 | 1656 | 806 | 864 |
| *hkl* range | -13/13, -16/16, -16/16 | -13/13, -17/17, -25/30 | -15/15, -16/11, -17/17 | -22/20, -12/12, -22/22 |
| Reflections collected | 17230 | 22375 | 26137 | 39814 |
| Independent reflections | 7618 | 7538 | 7747 | 6522 |
| $R_{int.}$ | 0.1633 | 0.0450 | 0.0503 | 0.0655 |
| No. parameters | 418 | 436 | 414 | 212 |
| $R_1$ [I≥2$\sigma$(*I*)] | 0.0686 | 0.0659 | 0.0567 | 0.0457 |
| $wR_2$ (all data) | 0.1599 | 0.1359 | 0.1520 | 0.1194 |
| Goodness-of-fit | 0.788 | 1.256 | 1.095 | 1.022 |
| Absolute structure parameter | | 0.003(9) | | |
| $\Delta\rho_{fin}$ max/min [eÅ$^{-3}$] | 1.093/-1-035 | 0.844/-0.580 | 1.301/-1.183 | 0.906/-1.253 |

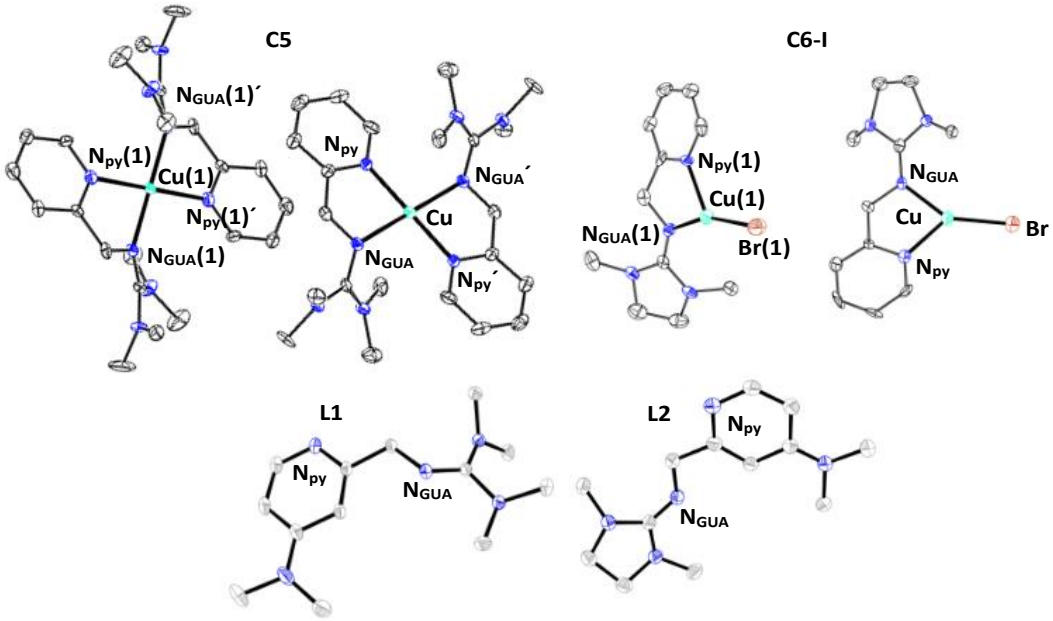


**Fig. S3** Molecular structure of the cationic complex unit in crystals of $[Cu(TMGpy)_2]Br_2$ (**C5**) and of the ligand or the complex in crystals of $TMGm4NMe_2py$ (**L1**), $DMEGm4NMe_2py$ (**L2**), and [Cu(DMEGpy)Br] (**C6-I**) in the solid state (ellipsoids drawn at the 50% probability level). H atoms and solvent molecules are omitted for clarity. In C5 and C6-I two independent molecules per asymmetric unit are present.

**Table S3** Crystallographic data and parameters of the Cu(II) complex $[Cu(TMGpy)_2]Br_2$ (**C5**), of the Cu(I) complex [Cu(DMEGpy)Br] (**C6-I**) and of the ligands $TMGm4NMe_2py$ (**L1**) and $DMEGm4NMe_2py$ (**L2**).

| Complex | **C5** | **C6-I** | **L1** | **L2** |
|---|---|---|---|---|
| Empirical formula | $C_{22}H_{36}Br_2CuN_8$ | $C_{11}H_{16}BrCuN_4$ | $C_{13}H_{23}N_5$ | $C_{13}H_{21}N_5$ |
| Formula mass [g mol$^{-1}$] | 635.95 | 347.73 | 249.36 | 247.35 |
| Crystal size [mm] | 0.25 x 0.12 x 0.09 | 0.24 x 0.07 x 0.06 | 0.16 x 0.14 x 0.12 | 0.22 x 0.13 x 0.08 |
| T [K] | 173(2) | 173(2) | 100(2) | 100(2) |
| Crystal system | Triclinic | Monoclinic | Monoclinic | Monoclinic |
| Space group | $P\bar{1}$ | $P2_1/c$ | $P2_1/c$ | $P2_1/c$ |
| a [Å] | 9.0168(7) | 13.9718(8) | 7.7101(15) | 7.2681(15) |
| b [Å] | 9.9820(7) | 8.0130(6) | 8.2333(16) | 12.646(3) |
| c [Å] | 14.8745(10) | 23.5855(15) | 21.676(4) | 14.978(3) |
| α [°] | 77.378(6) | 90 | 90 | 90 |
| β [°] | 86.558(6) | 99.071(6) | 94.89(3) | 103.60(3) |
| γ [°] | 87.412(6) | 90 | 90 | 90 |
| V [Å$^3$] | 1303.37(16) | 2607.5(3) | 1371.0(5) | 1338.1(5) |
| Z | 2 | 8 | 4 | 4 |
| $\rho_{calcd.}$ [g cm$^{-3}$] | 1.620 | 1.772 | 1.208 | 1.228 |
| μ [mm$^{-1}$] | 3.930 | 4.723 | 0.076 | 0.612 |
| λ [Å] | 0.71073 | 0.71073 | 0.71073 | 1.54186 |
| F(000) | 646 | 1392 | 544 | 536 |
| *hkl* range | -10/10, -12/11, -18/17 | -16/16, -9/9, -28/28 | -11/6, -12/11, -30/32 | -8/8, -10/15, -17/12 |
| Reflections collected | 11081 | 20124 | 13904 | 6480 |
| Independent reflections | 4817 | 4842 | 4924 | 2369 |
| $R_{int.}$ | 0.0443 | 0.0655 | 0.0311 | 0.0210 |
| No. parameters | 309 | 311 | 169 | 167 |
| $R_1$ [I≥2σ(*I*)] | 0.0544 | 0.0353 | 0.0556 | 0.0441 |
| $wR_2$ (all data) | 0.1783 | 0.0443 | 0.1520 | 0.1313 |
| Goodness-of-fit | 1.188 | 0.830 | 1.081 | 1.073 |
| $\Delta\rho_{fin}$ max/min [eÅ$^{-3}$] | 1.378/-0.699 | 0.923/-0.659 | 0.417/-0.275 | 0.249/-0.245 |

**Table S4**: Key bond lengths, angles and geometrical factors of the complexes $[Cu(TMGqu)_2Br]Br$,[1] $[Cu(TMGqu)_2]Br$,[1] $[Cu(DMEGqu)_2Br]Br$[1] and $[Cu(DMEGqu)_2]Br$.[1]

| Complex | $[Cu(TMGqu)_2Br]Br$ | $[Cu(TMGqu)_2]Br$ | $[Cu(DMEGqu)_2Br]Br$ | $[Cu(DMEGqu)_2]Br$ |
|---|---|---|---|---|
| **Bond lengths [Å]** | | | | |
| Cu-$N_{GUA}$ (L1) | 2.051(7) | 2.118(2) | 2.052(5) | 2.101(2) |
| Cu-$N_{GUA}$ (L2) | 2.052(7) | 2.125(2) | 2.125(4) | 2.116(2) |
| Cu-$N_{qu}$ (L1) | 1.971(7) | 1.987(2) | 1.958(5) | 1.968(3) |
| Cu-$N_{qu}$ (L2) | 1.979(7) | 1.974(2) | 1.956(4) | 1.963(3) |
| Cu-Br (1) | 2.663(2) | - | 2.593(1) | - |
| $C_{GUA}$=$N_{GUA}$ (L1) | 1.34(2) | 1.326(2) | 1.349(7) | 1.318(4) |
| $C_{GUA}$-$N_{am}$ (L1) (Ø) | 1.35(2) | 1.363(2) | 1.336(8) | 1.352(4) |
| $C_{GUA}$=$N_{GUA}$ (L2) | 1.37(2) | 1.327(2) | 1.341(8) | 1.314(4) |
| $C_{GUA}$-$N_{am}$ (L2) (Ø) | 1.35(2) | 1.356(2) | 1.341(9) | 1.353(4) |
| **Bond angles [°]** | | | | |
| $N_{GUA}$ (L1)-Cu-$N_{GUA}$ (L2) | 131.4(3) | 127.0(1) | 127.8(1) | 127.8(1) |
| $N_{qu}$ (L1)-Cu-$N_{qu}$ (L2) | 174.8(3) | 150.9(1) | 178.7(2) | 153.8(1) |
| $N_{GUA}$ (L1)-Cu-Br (1) | 127.4(2 | - | 137.8(2) | - |
| **Geometrical factors** | | | | |
| $\tau_4$[a] | - | 0.58 | - | 0.55 |
| $\tau_5$[b] | 0.72 | - | 0.68 | - |
| $\rho$[c] | 1.01 | 0.98 | 1.01 | 0.97 |
| ∢ (CuN2 (L1/L2)) [°] | 50.2(2) | 65.6(1) | 57.0(2) | 63.5(1) |

[a] $\tau_4 = \frac{360°-(\alpha+\beta)}{141}$. A $\tau_4$ value of 0 is found in ideal square planar complexes where a $\tau_4$ value of 1 is found in ideal tetrahedral complexes.[2]

[b] $\tau_5 = \frac{(\alpha-\beta)}{60}$. A $\tau_5$ value of 0 is found in ideal square-based pyramidal complexes where a $\tau_5$ value of of 1 is found in ideal trigonal bipyramidal complexes.[3]

[c] $\rho = \frac{2a}{(b+c)}$ with a = d($C_{GUA}$=$N_{GUA}$) and b and c = d($C_{GUA}$=$N_{am}$). Average $\rho$-values of two guanidine moieties.[4]

## Cyclic voltammogramms

**Table S5** Additional data and parameters to the cyclic voltammograms of the $[Cu(TMGm4NMe_2py)_2]^+/[Cu(TMGm4NMe_2py)_2]^{2+}$ couple starting from a 1 mM $[Cu(TMGm4NMe_2py)_2]Br_2$ (**C1-B**) complex solution in MeCN.

| | 20 mV/s | 50 mV/s | 100 mV/s | 200 mV/s |
|---|---|---|---|---|
| $E_{ox}$ vs. SCE [V] | -0,422 | -0,418 | -0,414 | -0,410 |
| $E_{red}$ vs. SCE [V] | -0,509 | -0,519 | -0,525 | -0,535 |
| $E_{1/2}$ vs. SCE [V] | -0,465 | -0,468 | -0,469 | -0,472 |
| $\Delta E$ [V] | 0,087 | 0,101 | 0,111 | 0,125 |
| $I_{ox}$ [A] | $8{,}53 \times 10^{-7}$ | $1{,}28 \times 10^{-6}$ | $1{,}68 \times 10^{-6}$ | $2{,}12 \times 10^{-6}$ |
| $I_{red}$ [A] | $-9{,}04 \times 10^{-7}$ | $-1{,}46 \times 10^{-6}$ | $-1{,}96 \times 10^{-6}$ | $-2{,}57 \times 10^{-6}$ |
| $I_{red}/I_{ox}$ | -1,06 | -1,14 | -1,17 | -1,21 |
| Current function (ox) [$\mu A\ V^{-0.5}\ s^{0.5}\ mmol^{-1}\ l$] | $6{,}03 \times 10^{-6}$ | $5{,}72 \times 10^{-6}$ | $5{,}30 \times 10^{-6}$ | $4{,}75 \times 10^{-6}$ |
| Current function (red) [$\mu A\ V^{-0.5}\ s^{0.5}\ mmol^{-1}\ l$] | $-6{,}39 \times 10^{-6}$ | $-6{,}53 \times 10^{-6}$ | $-6{,}21 \times 10^{-6}$ | $-5{,}74 \times 10^{-6}$ |

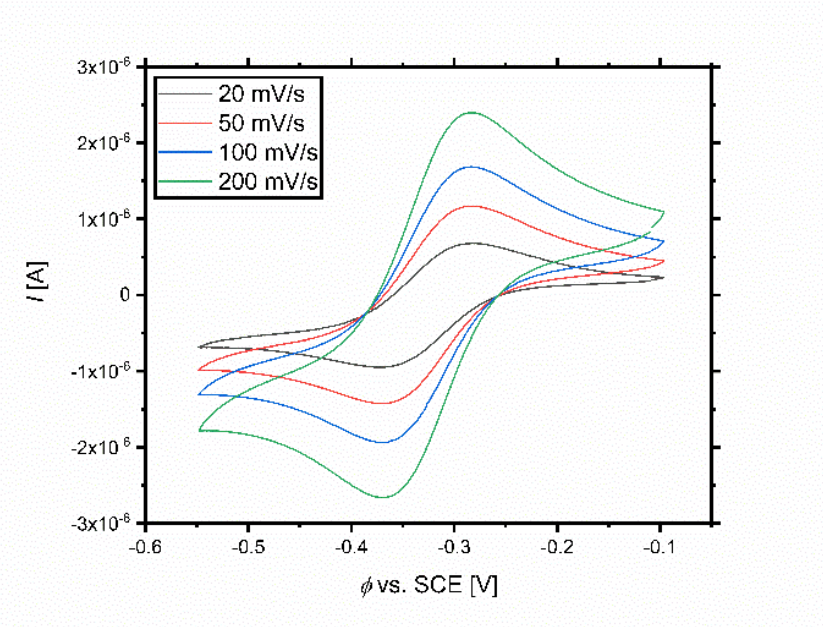


**Fig. S4** Cyclic voltammograms with various scan rates of the $[Cu(DMEGm4NMe_2py)_2]^+/[Cu(DMEGm4NMe_2py)_2]^{2+}$ couple starting from a 1 mM $[Cu(DMEGm4NMe_2py)_2Br]Br$ (**C2**) complex solution in MeCN.

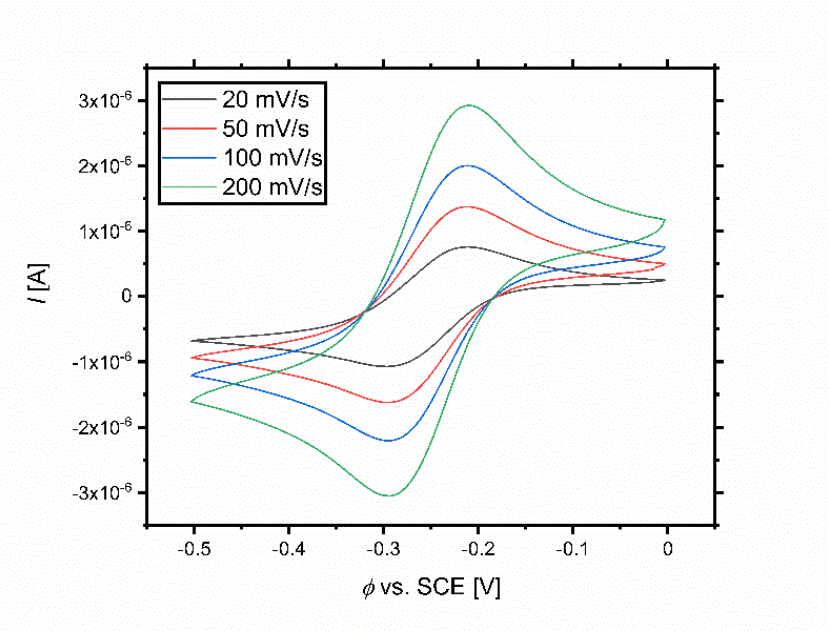


**Fig. S5** Cyclic voltammograms with various scan rates of the $[Cu(TMG4NMe_2qu)_2]^+/[Cu(TMG4NMe_2qu)_2]^{2+}$ couple starting from a 1 mM $[Cu(TMG4NMe_2qu)_2Br]Br$ (**C3**) complex solution in MeCN.

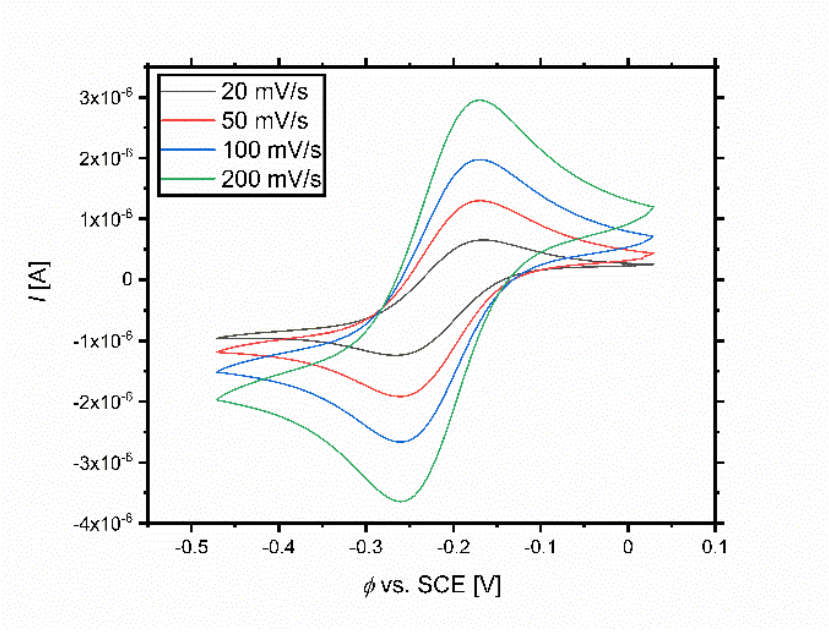


**Fig. S6** Cyclic voltammograms with various scan rates of the $[Cu(DMEG4NMe_2qu)_2]^+/[Cu(DMEG4NMe_2qu)_2]^{2+}$ couple starting from a 1 mM $[Cu(DMEG4NMe_2qu)_2Br]Br$ (**C4**) complex solution in MeCN.

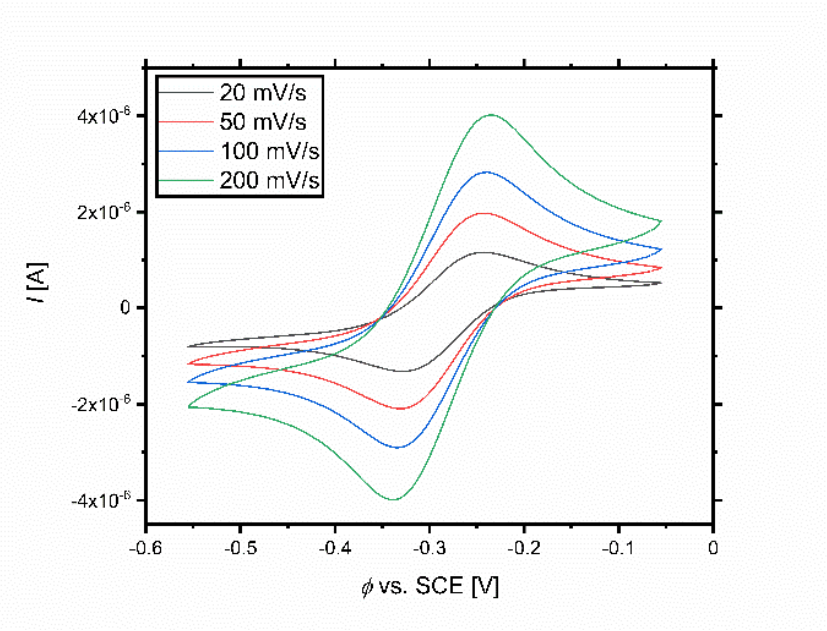


**Fig. S7** Cyclic voltammograms with various scan rates of the $[Cu(TMGpy)_2]^+/[Cu(TMGpy)_2]^{2+}$ couple starting from a 1 mM $[Cu(TMGpy)_2]Br_2$ (**C5**) complex solution in MeCN.

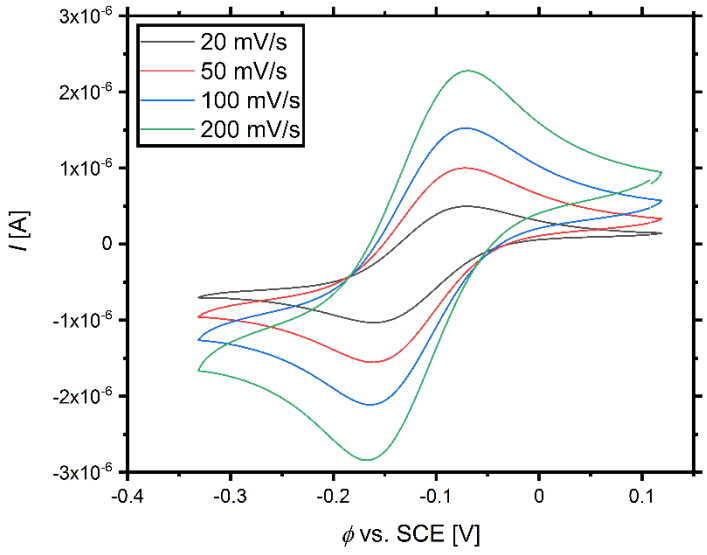


**Fig. S8** Cyclic voltammograms with various scan rates of the $[Cu(DMEGpy)_2]^+/[Cu(DMEGpy)_2]^{2+}$ couple starting from a 1 mM $[Cu(DMEGpy)_2Br]Br$ (**C6**) complex solution in MeCN.

## Polymerisation kinetics

### Standard ATRP experiments

**Table S6** Used amounts of chemicals and ratios for standard ATRP experiments of styrene in benzonitrile.

| | Ligand | CuBr | EBiB | Styrene | Ratio (C/I/M) |
|---|---|---|---|---|---|
| **L1** | 0.38 mmol | 0.19 mmol | 0.19 mmol | 19 mmol | 1/1/100 |
| **L1** | 0.19 mmol | 0.095 mmol | 0.19 mmol | 19 mmol | 0.5/1/100 |
| **L1** | 0.038 mmol | 0.19 mmol | 0.19 mmol | 19 mmol | 0.1/1/100 |
| **L2** | 0.38 mmol | 0.19 mmol | 0.19 mmol | 19 mmol | 1/1/100 |
| **L2** | 0.19 mmol | 0.095 mmol | 0.19 mmol | 19 mmol | 0.5/1/100 |
| **L2** | 0.038 mmol | 0.19 mmol | 0.19 mmol | 19 mmol | 0.1/1/100 |
| **L3** | 0.38 mmol | 0.19 mmol | 0.19 mmol | 19 mmol | 1/1/100 |
| **L3** | 0.19 mmol | 0.095 mmol | 0.19 mmol | 19 mmol | 0.5/1/100 |
| **L4** | 0.38 mmol | 0.19 mmol | 0.19 mmol | 19 mmol | 1/1/100 |
| **L4** | 0.19 mmol | 0.095 mmol | 0.19 mmol | 19 mmol | 0.5/1/100 |

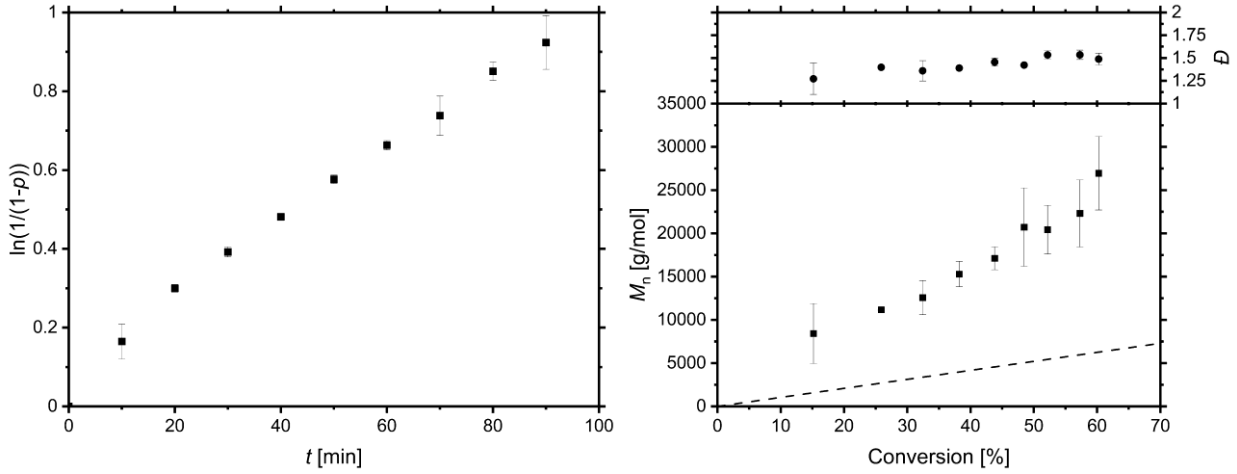


**Fig. S9** Semilogarithmic plot of conversion vs. time (left) and $M_n$/$Đ$ vs. conversion (right) for styrene ATRP experiments with the CuBr/(TMGm4NMe$_2$py)$_2$ catalyst system. Conditions: Styrene/EBiB/Cat. = 100/1/1 in benzonitrile at 110 °C.

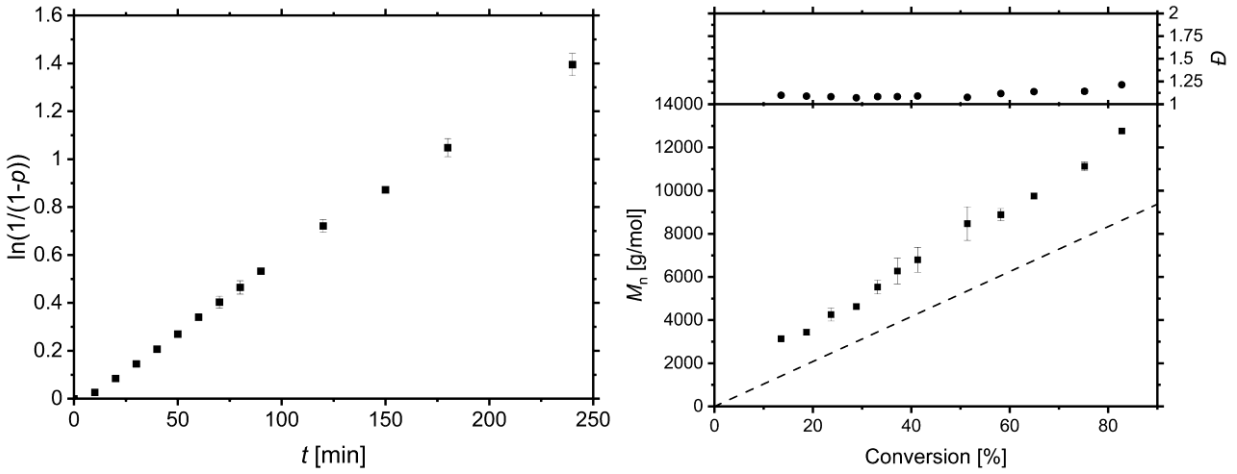


**Fig. S10** Semilogarithmic plot of conversion vs. time (left) and $M_n$/$Đ$ vs. conversion (right) for styrene ATRP experiments with the CuBr/(TMGm4NMe$_2$py)$_2$ catalyst system. Conditions: Styrene/EBiB/Cat. = 100/1/0.5 in benzonitrile at 110 °C.

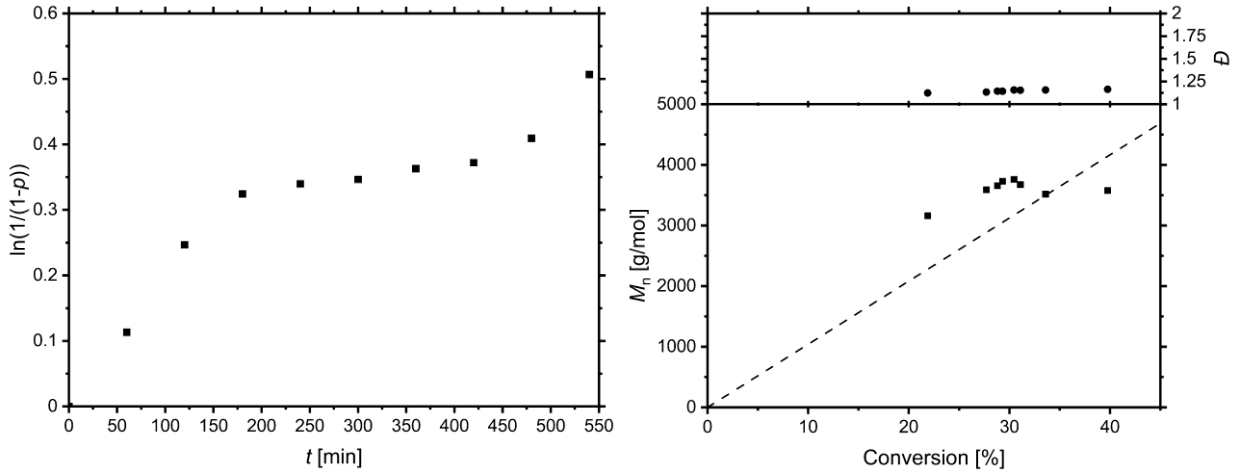


**Fig. S11** Semilogarithmic plot of conversion vs. time (left) and $M_n$/$Đ$ vs. conversion (right) for styrene ATRP experiments with the CuBr/(TMGm4NMe$_2$py)$_2$ catalyst system. Conditions: Styrene/EBiB/Cat. = 100/1/0.1 in benzonitrile at 110 °C.

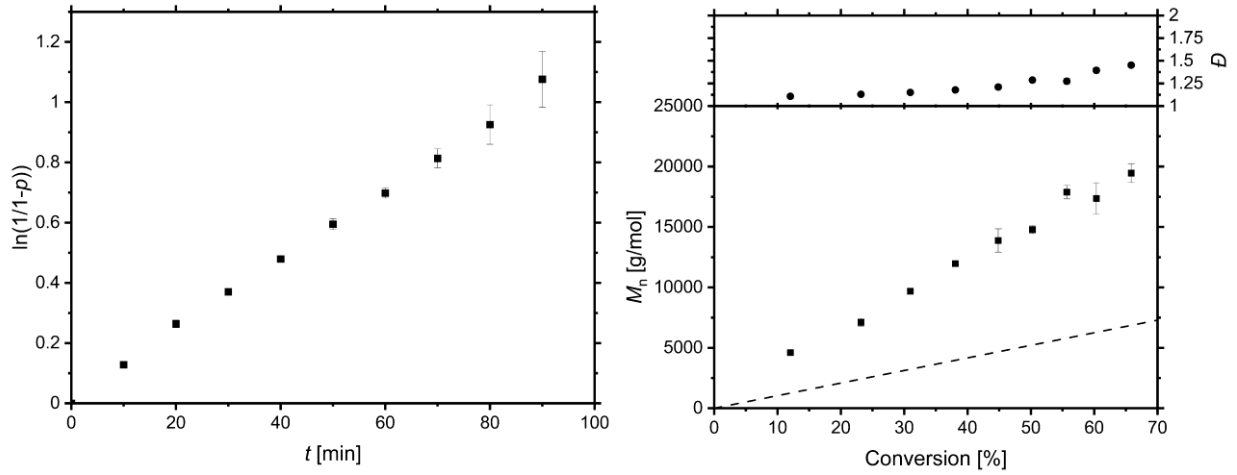


**Fig. S12** Semilogarithmic plot of conversion vs. time (left) and $M_n$/$Đ$ vs. conversion (right) for styrene ATRP experiments with the CuBr/(DMEGm4NMe$_2$py)$_2$ catalyst system. Conditions: Styrene/EBiB/Cat. = 100/1/1 in benzonitrile at 110 °C.

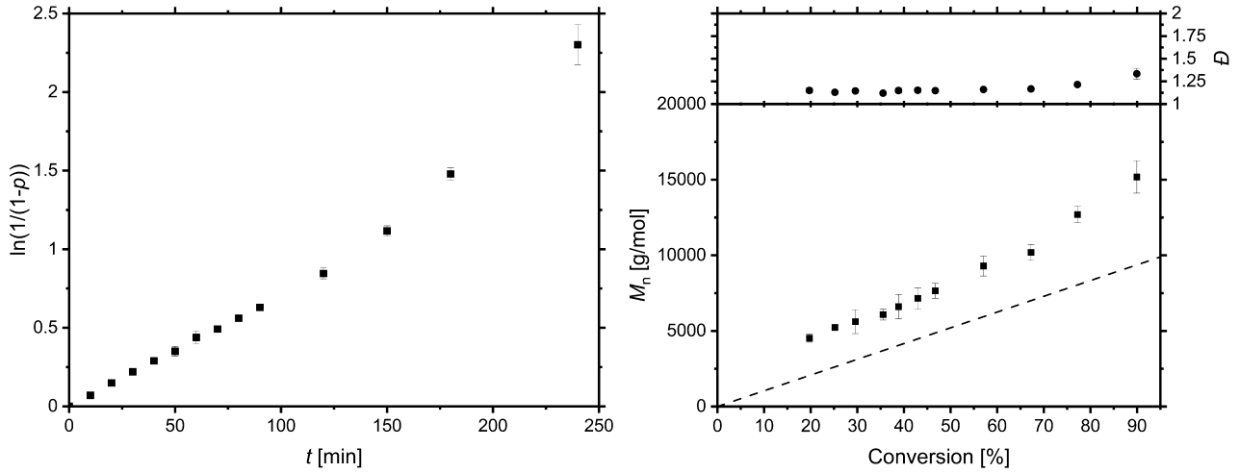


**Fig. S13** Semilogarithmic plot of conversion vs. time (left) and $M_n$/$Đ$ vs. conversion (right) for styrene ATRP experiments with the CuBr/(DMEGm4NMe$_2$py)$_2$ catalyst system. Conditions: Styrene/EBiB/Cat. = 100/1/0.5 in benzonitrile at 110 °C.

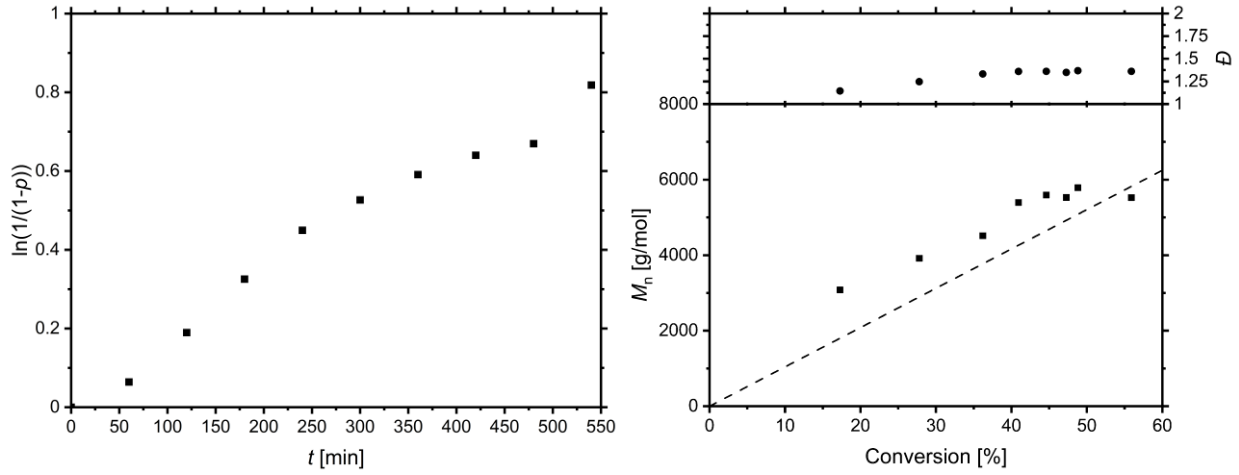


**Fig. S14** Semilogarithmic plot of conversion vs. time (left) and $M_n$/$Đ$ vs. conversion (right) for styrene ATRP experiments with the CuBr/(DMEGm4NMe$_2$py)$_2$ catalyst system. Conditions: Styrene/EBiB/Cat. = 100/1/0.1 in benzonitrile at 110 °C.

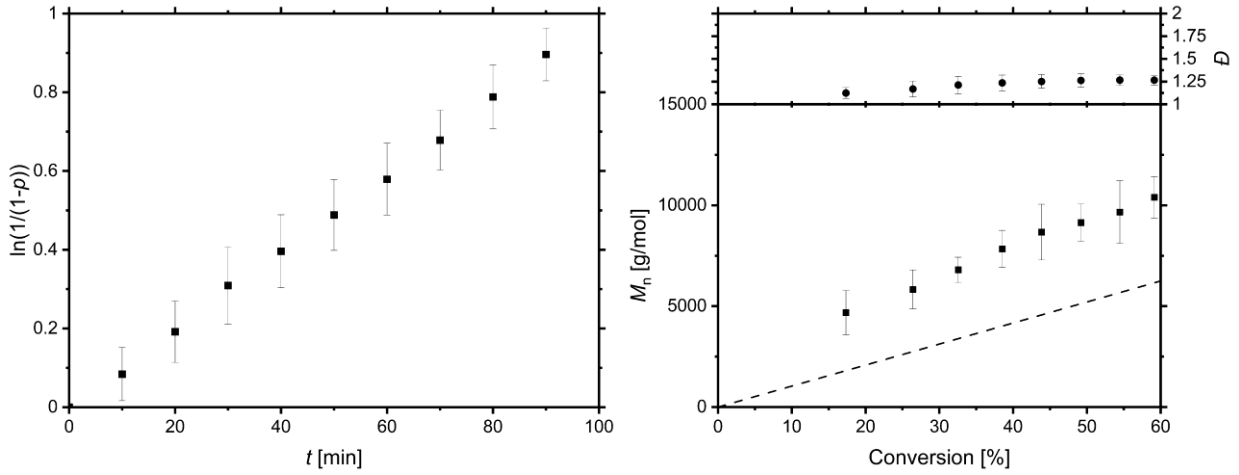


**Fig. S15** Semilogarithmic plot of conversion vs. time (left) and $M_n$/$Đ$ vs. conversion (right) for styrene ATRP experiments with the CuBr/(TMG4NMe$_2$qu)$_2$ catalyst system. Conditions: Styrene/EBiB/Cat. = 100/1/1 in benzonitrile at 110 °C.

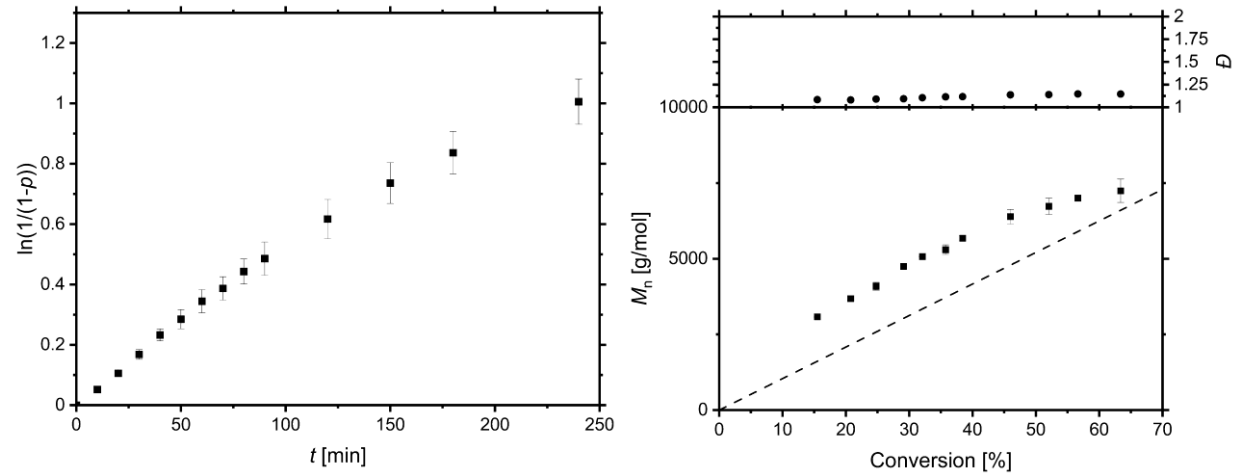


**Fig. S16** Semilogarithmic plot of conversion vs. time (left) and $M_n$/$Đ$ vs. conversion (right) for styrene ATRP experiments with the CuBr/(TMG4NMe$_2$qu)$_2$ catalyst system. Conditions: Styrene/EBiB/Cat. = 100/1/0.5 in benzonitrile at 110 °C.

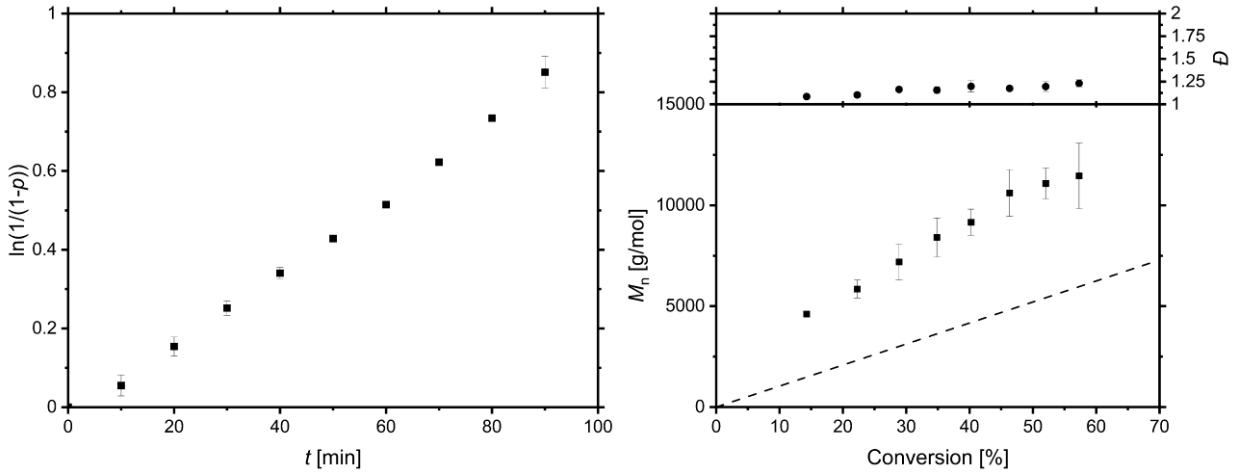


**Fig. S17** Semilogarithmic plot of conversion vs. time (left) and $M_n$/Đ vs. conversion (right) for styrene ATRP experiments with the CuBr/(DMEG4NMe$_2$qu)$_2$ catalyst system. Conditions: Styrene/EBiB/Cat. = 100/1/1 in benzonitrile at 110 °C.

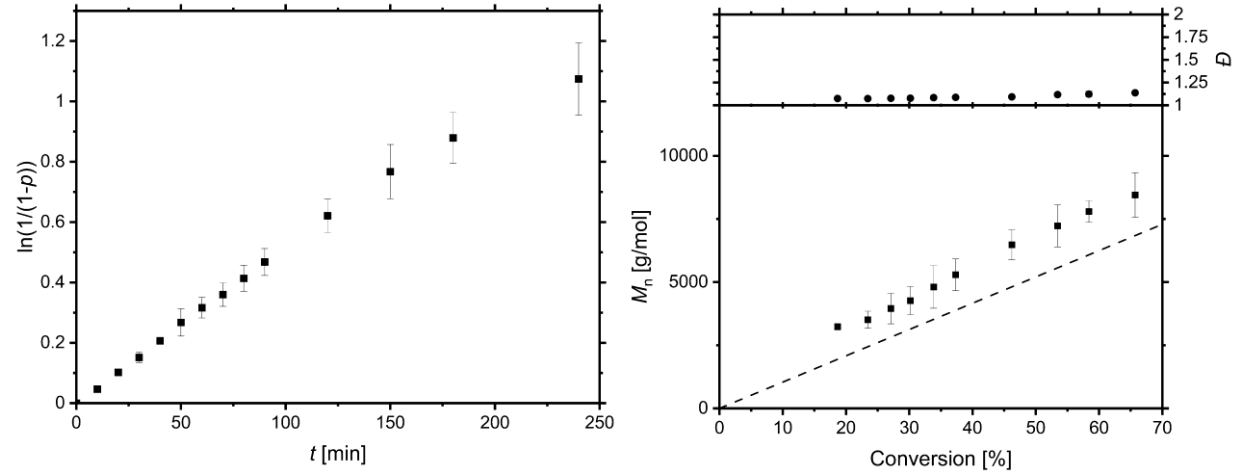


**Fig. S18** Semilogarithmic plot of conversion vs. time (left) and $M_n$/Đ vs. conversion (right) for styrene ATRP experiments with the CuBr/(DMEG4NMe$_2$qu)$_2$ catalyst system. Conditions: Styrene/EBiB/Cat. = 100/1/0.5 in benzonitrile at 110 °C.

## ICAR ATRP experiments

**Table S7** Used amounts of chemicals and ratios for ICAR ATRP experiments of styrene in benzonitrile.

| | Ligand | $CuBr_2$ | EBiB | Styrene | AIBN | Ratio (C/I/M/AIBN) |
|---|---|---|---|---|---|---|
| **L1**[a] | 0.19 mmol | 0.095 mmol | 0.19 mmol | 19 mmol | 0.285 mmol | 0.5/1/100/1.5 |
| **L1**[a] | 0.038 mmol | 0.19 mmol | 0.19 mmol | 19 mmol | 0.285 mmol | 0.1/1/100/1.5 |
| **L1**[b] | 0.038 mmol | 0.19 mmol | 0.19 mmol | 19 mmol | 0.285 mmol | 0.1/1/100/1.5 |
| **L2**[a] | 0.038 mmol | 0.19 mmol | 0.19 mmol | 19 mmol | 0.285 mmol | 0.1/1/100/1.5 |
| **L2**[b] | 0.038 mmol | 0.19 mmol | 0.19 mmol | 19 mmol | 0.285 mmol | 0.1/1/100/1.5 |
| - | - | - | 0.19 mmol | 19 mmol | 0.285 mmol | 0/1/100/1.5 |

[a] T = 60°C, [b] T = 110°C,

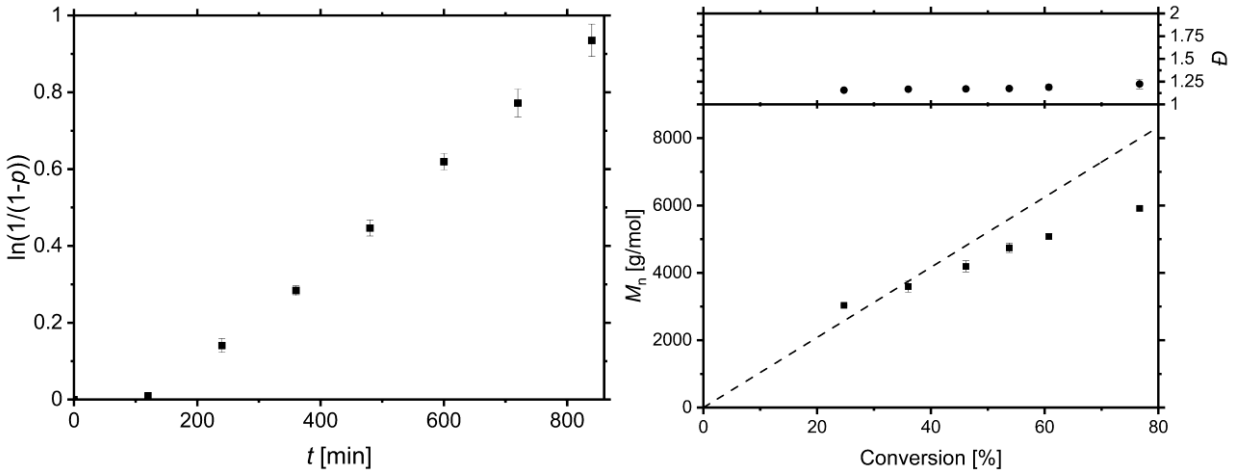


**Fig. S19** Semilogarithmic plot of conversion vs. time (left) and $M_n$/$Đ$ vs. conversion (right) for ICAR ATRP experiments of styrene with the $CuBr_2$/(TMGm4NMe$_2$py)$_2$ catalyst system. Conditions: Styrene/EBiB/Cat./AIBN = 100/1/0.5/1.5 in benzonitrile at 60 °C.

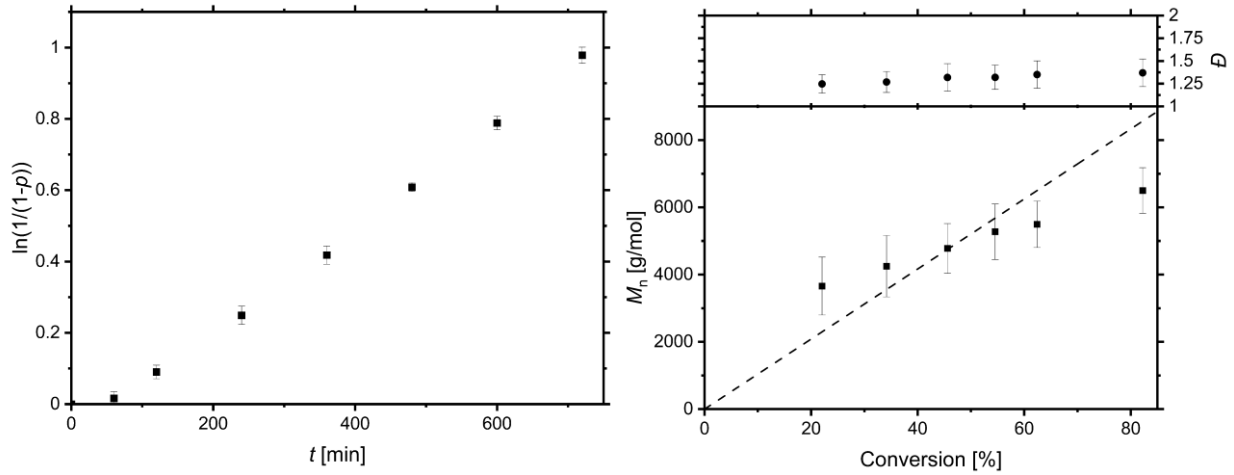


**Fig. S20** Semilogarithmic plot of conversion vs. time (left) and $M_n$/$Đ$ vs. conversion (right) for ICAR ATRP experiments of styrene with the $CuBr_2$/(TMGm4NMe$_2$py)$_2$ catalyst system. Conditions: Styrene/EBiB/Cat./AIBN = 100/1/0.1/1.5 in benzonitrile at 60 °C.

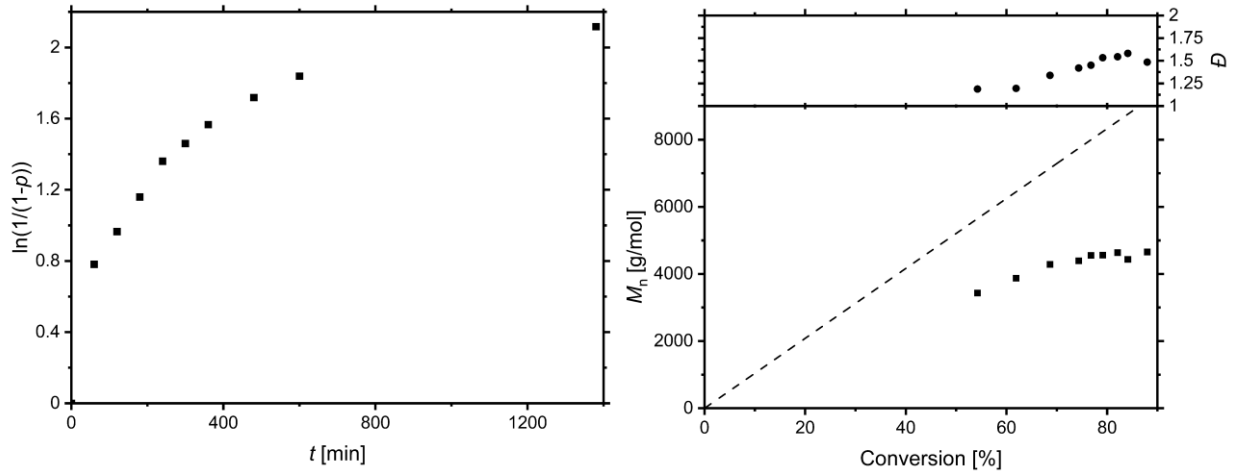


**Fig. S21** Semilogarithmic plot of conversion vs. time (left) and $M_n$/$Đ$ vs. conversion (right) for ICAR ATRP experiments of styrene with the $CuBr_2$/(TMGm4NMe$_2$py)$_2$ catalyst system. Conditions: Styrene/EBiB/Cat./AIBN = 100/1/0.1/1.5 in benzonitrile at 110 °C.

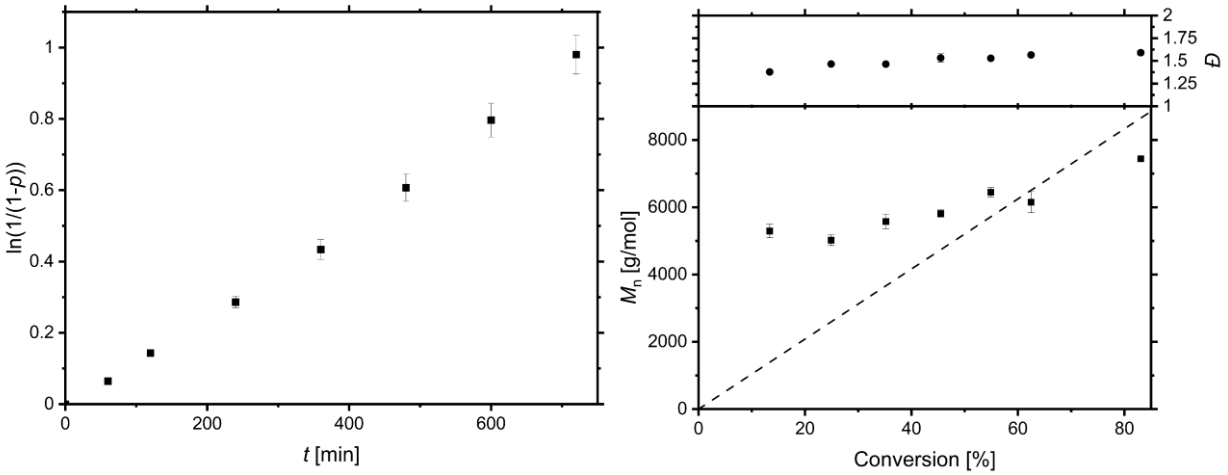


**Fig. S22** Semilogarithmic plot of conversion vs. time (left) and $M_n$/$Đ$ vs. conversion (right) for ICAR ATRP experiments of styrene with the $CuBr_2$/$(DMEGm4NMe_2py)_2$ catalyst system. Conditions: Styrene/EBiB/Cat./AIBN = 100/1/0.1/1.5 in benzonitrile at 60 °C.

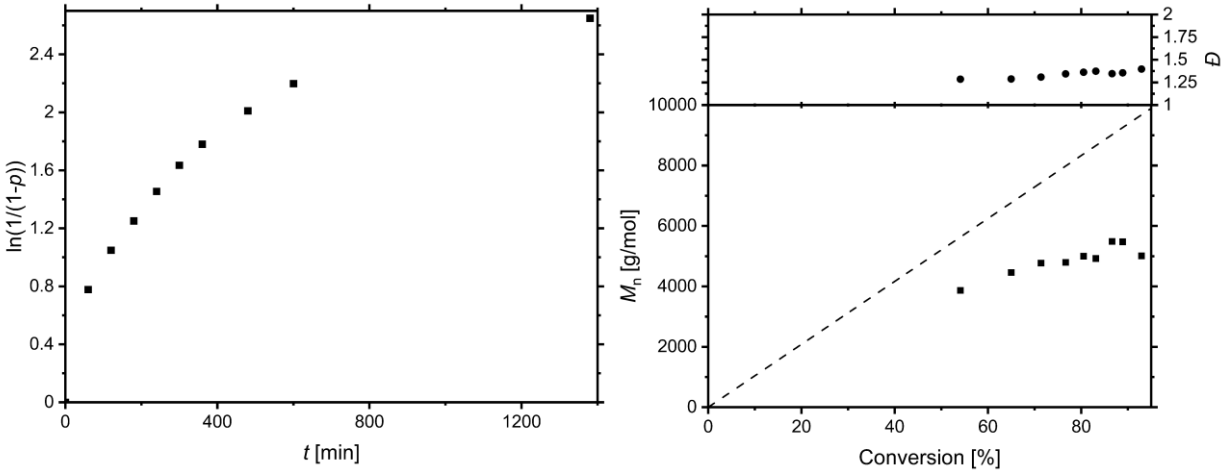


**Fig. S23** Semilogarithmic plot of conversion vs. time (left) and $M_n$/$Đ$ vs. conversion (right) for ICAR ATRP experiments of styrene with the $CuBr_2$/$(DMEGm4NMe_2py)_2$ catalyst system. Conditions: Styrene/EBiB/Cat./AIBN = 100/1/0.1/1.5 in benzonitrile at 110 °C.

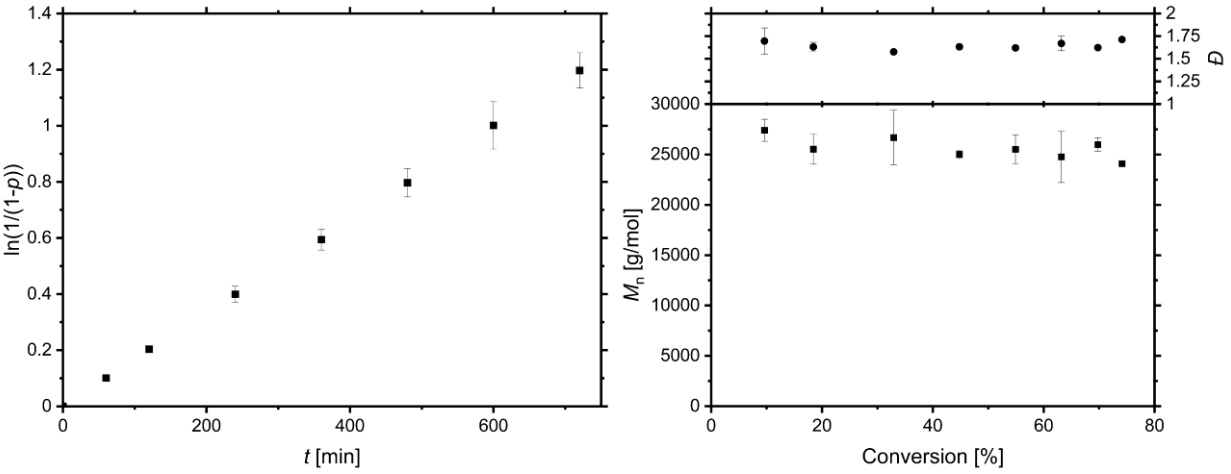


**Fig. S24** Semilogarithmic plot of conversion vs. time (left) and $M_n$/$Đ$ vs. conversion (right) for the ICAR ATRP reference experiment of styrene. Conditions: Styrene/EBiB/Cat./AIBN = 100/1/0/1.5 in benzonitrile at 60 °C.

## NMR-spectra

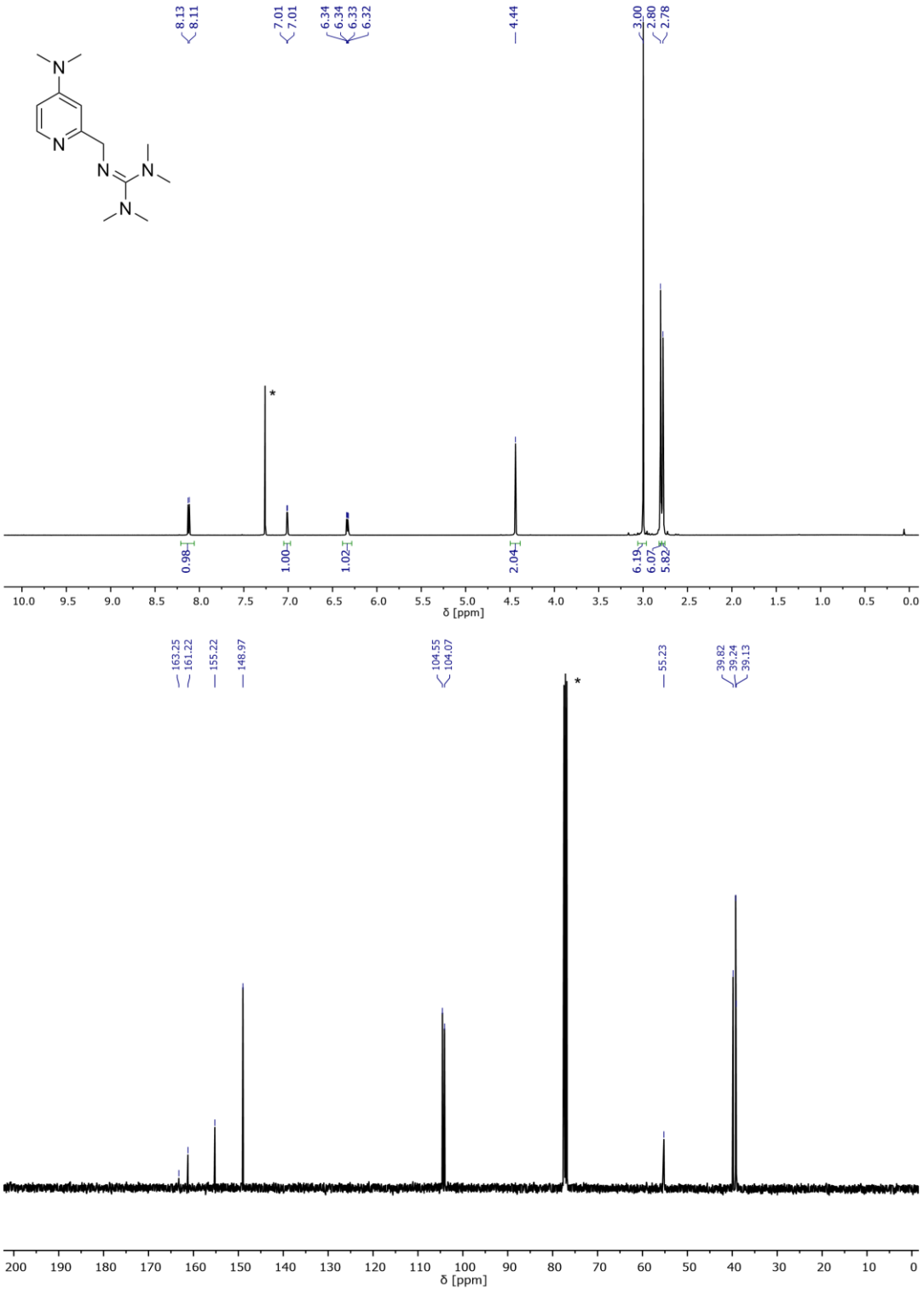


**Fig. S25** $^{1}$H-NMR (top) and $^{13}$C-NMR (bottom) spectrum for TMGm4NMe$_2$py (**L1**) in $CDCl_3$. *: $CDCl_3$.

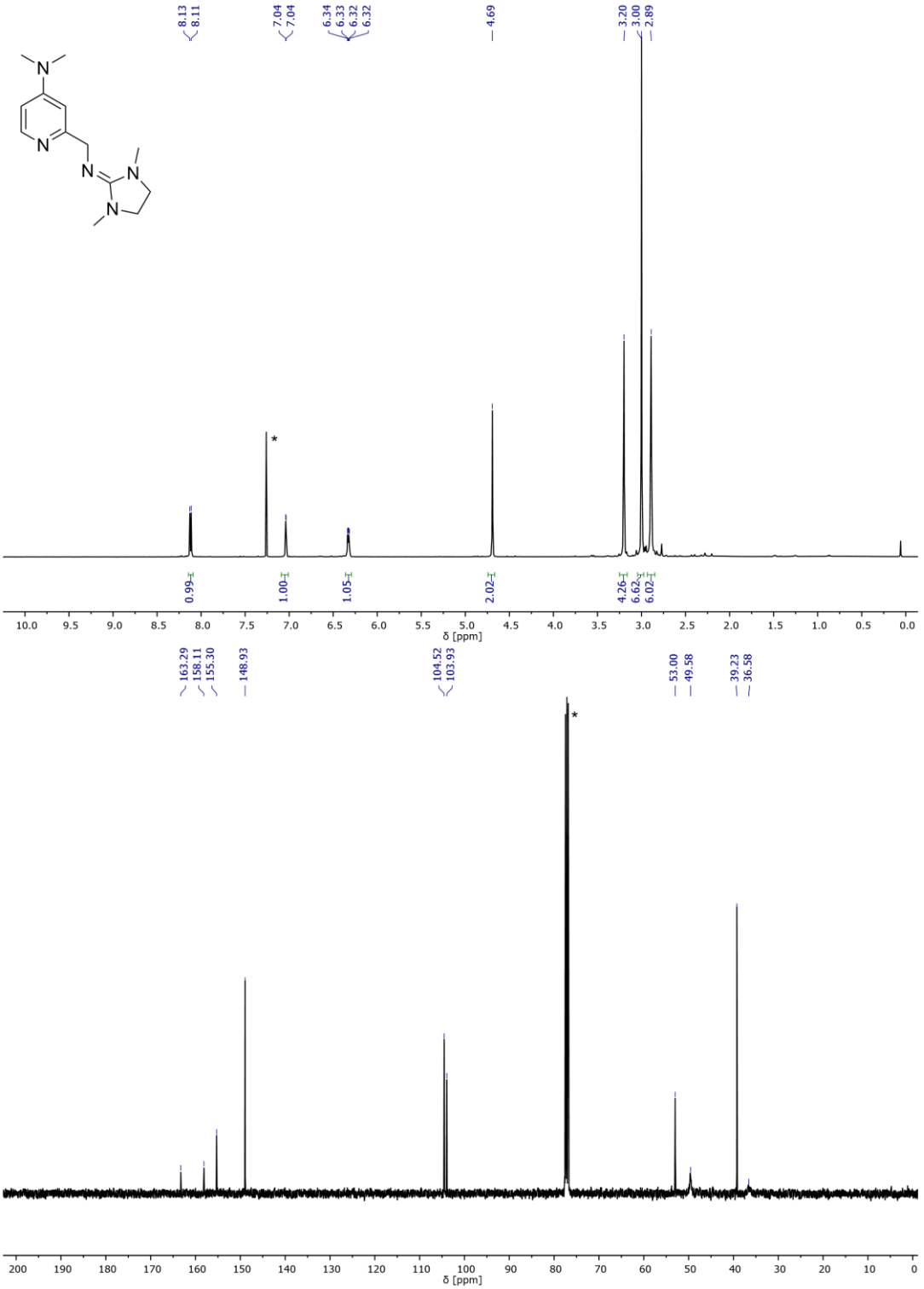


**Fig. S26** $^{1}$H-NMR (top) and $^{13}$C-NMR (bottom) spectrum for DMEGm4NMe$_2$py (**L2**) in $CDCl_3$. *: $CDCl_3$.

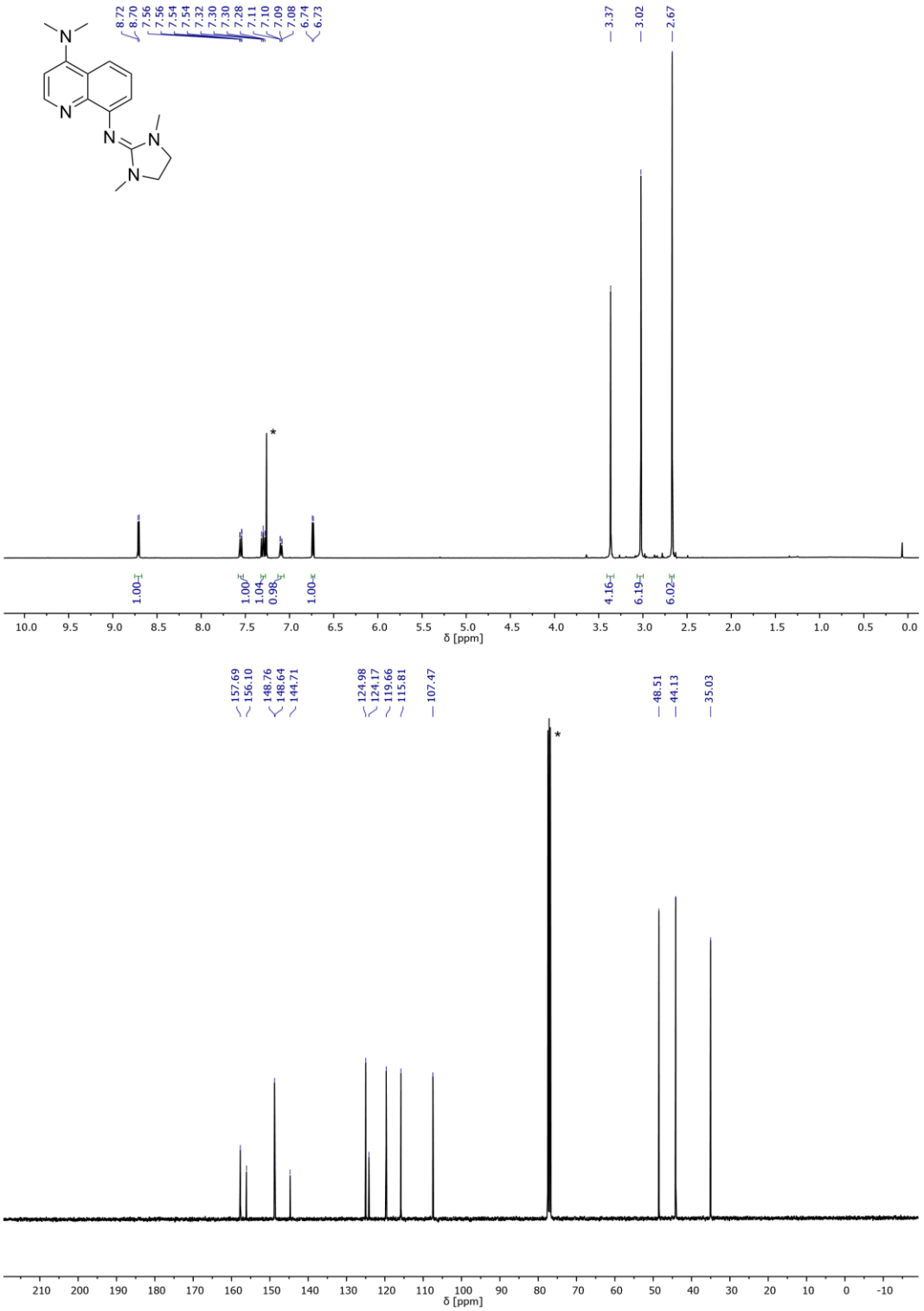


**Fig. S27** $^{1}$H-NMR (top) and $^{13}$C-NMR (bottom) spectrum for DMEG4NMe$_2$qu (**L4**) in $CDCl_3$. *: $CDCl_3$.

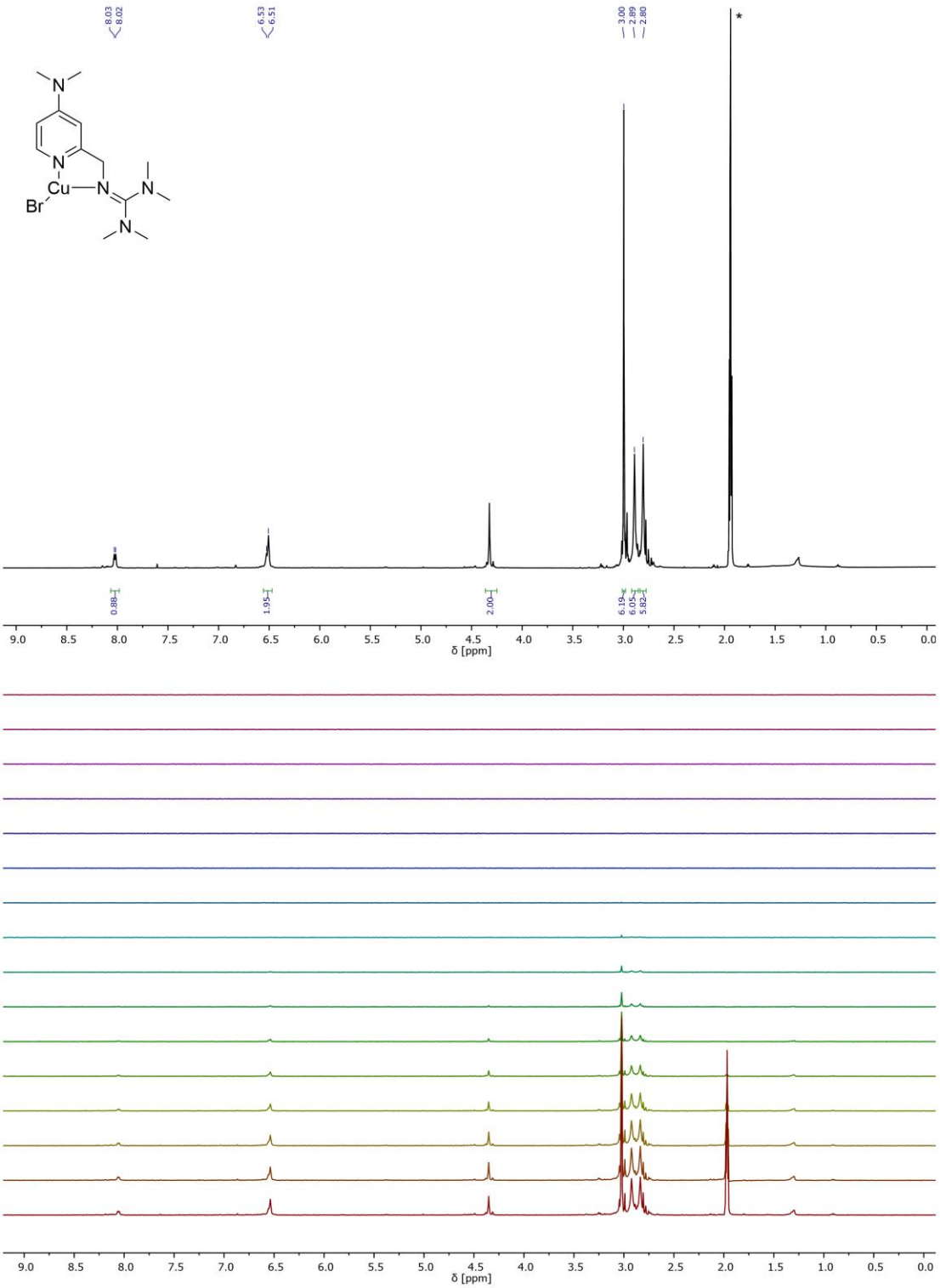


**Fig. S28** $^{1}$H-NMR spectrum (top) and DOSY spectrum (bottom) of the proposed complex structures of CuBr + 1 eq. TMGm4NMe$_2$py in MeCN-$d_3$. *: MeCN-d$_3$.

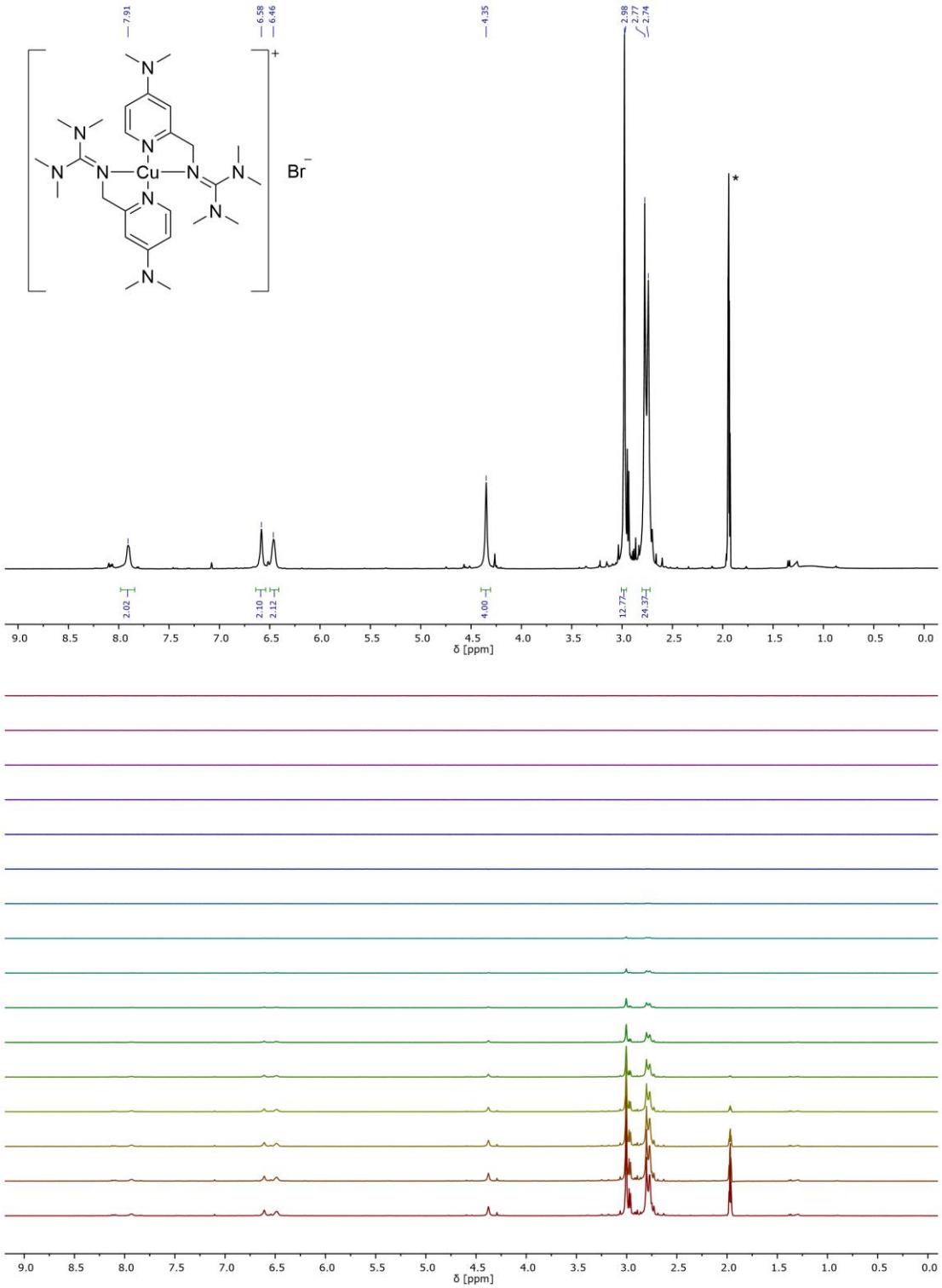


**Fig. S29** $^{1}$H-NMR spectrum (top) and DOSY spectrum (bottom) of the proposed complex structures of CuBr + 2 eq. TMGm4NMe$_2$py in MeCN-$d_3$. *: MeCN-d$_3$.

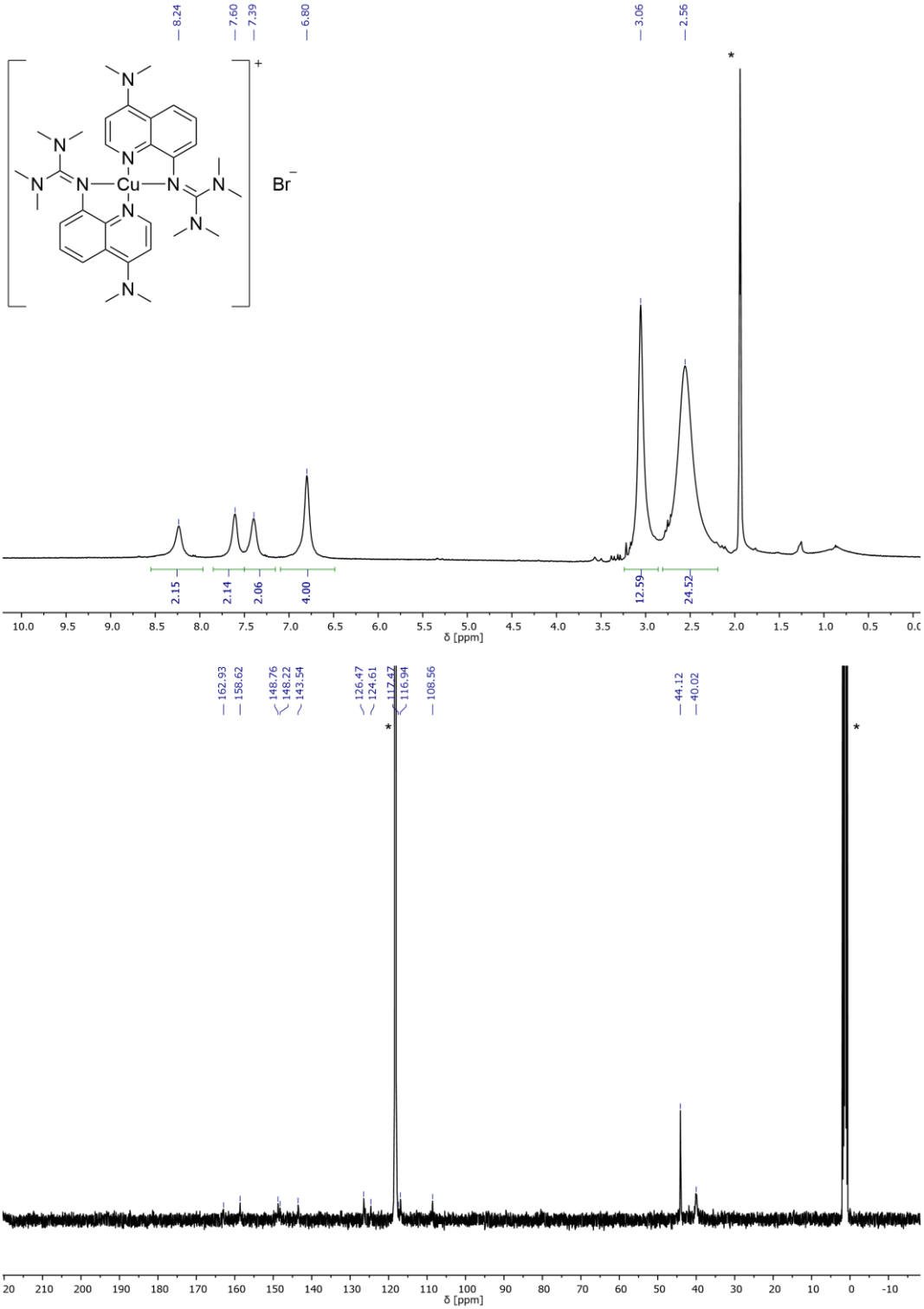


**Fig. S30** $^{1}$H-NMR (top) and $^{13}$C-NMR (bottom) spectrum for [Cu(TMG4NMe$_2$qu)$_2$]Br (**C3-I**) in MeCN-$d_3$. *: MeCN-d$_3$.

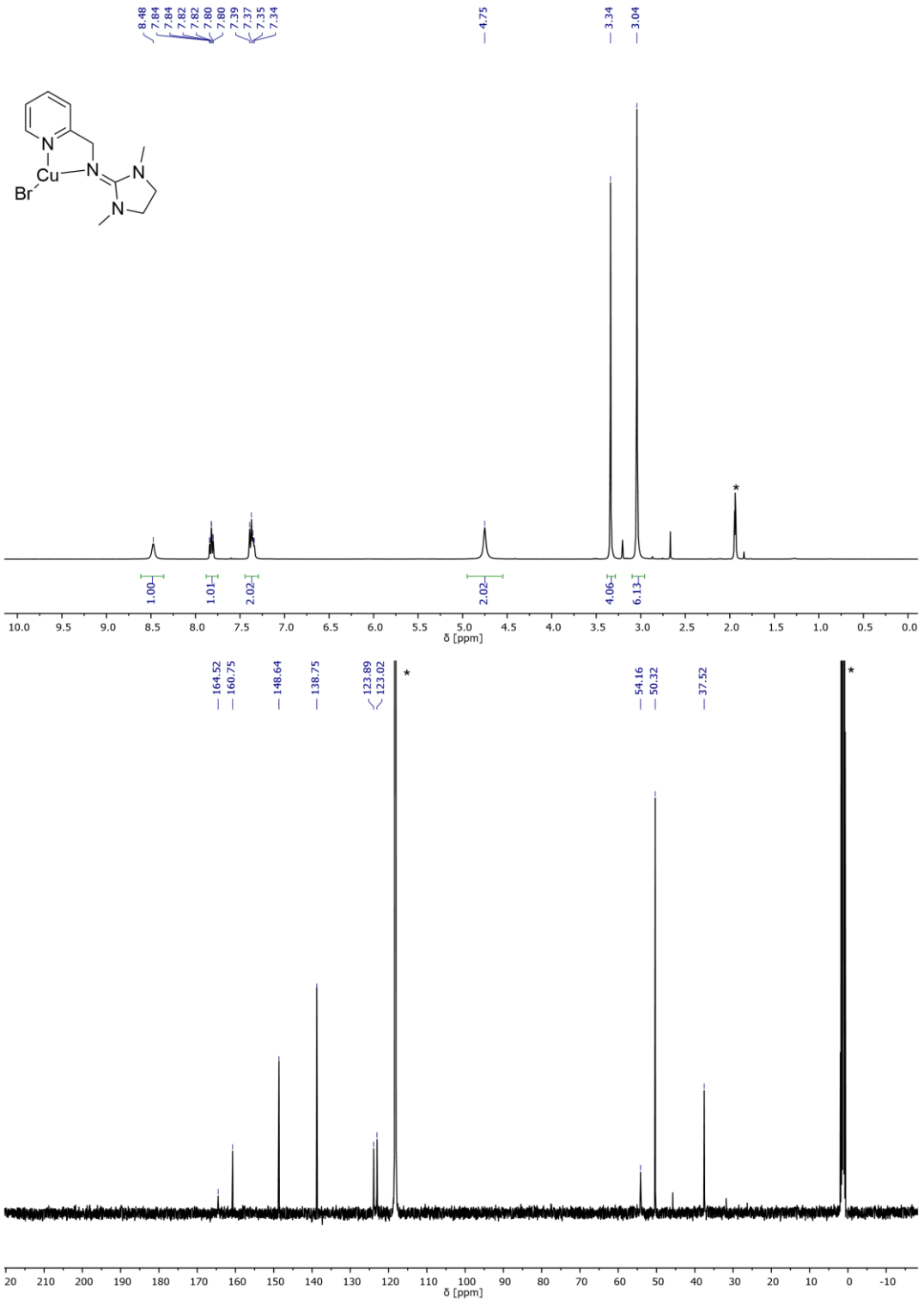


**Fig. S31** $^{1}$H-NMR (top) and $^{13}$C-NMR (bottom)spectrum for [Cu(DMEGpy)Br] (**C6-I**) in MeCN-$d_3$. *: MeCN-$d_3$.

## UV/Vis spectra

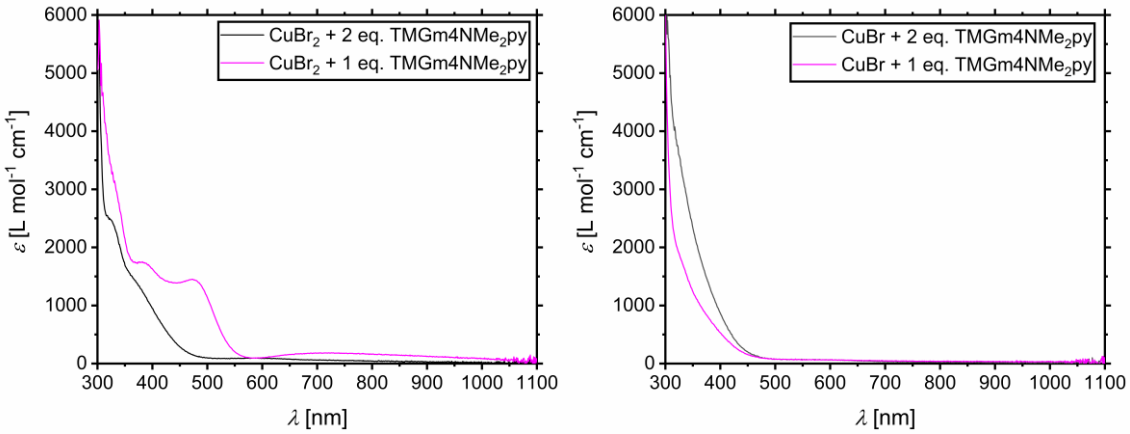


**Fig. S32** UV/Vis spectra of 5 mM $CuBr_2$ (left) and CuBr (right) in MeCN with one or two added equivalents of $TMGm4NMe_2py$ (**L1**).

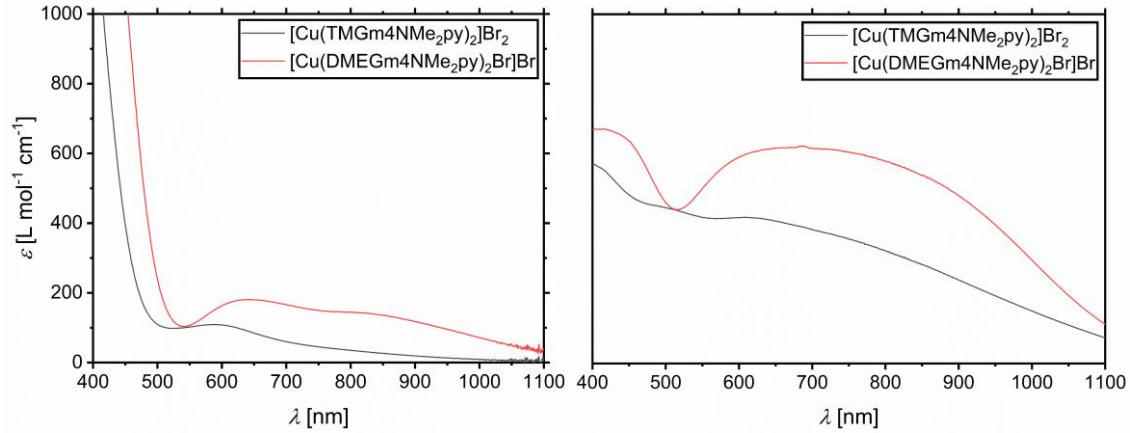


**Fig. S33** UV/Vis spectra of 2.5 mM **C1-B** and **C2** complex solutions in MeCN (left) and in the solid state (right).

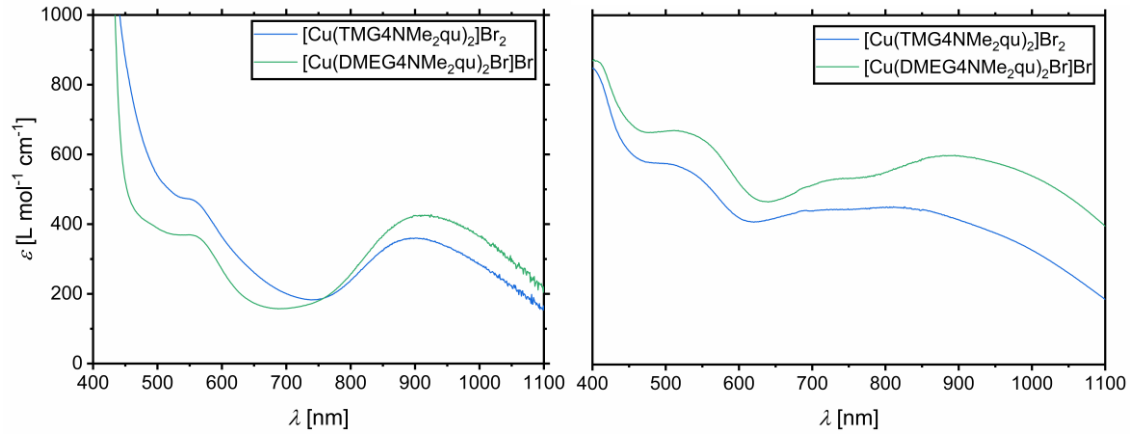


**Fig. S34** UV/Vis spectra of 2.5 mM **C3** and **C4** complex solutions in MeCN (left) and in the solid state (right).

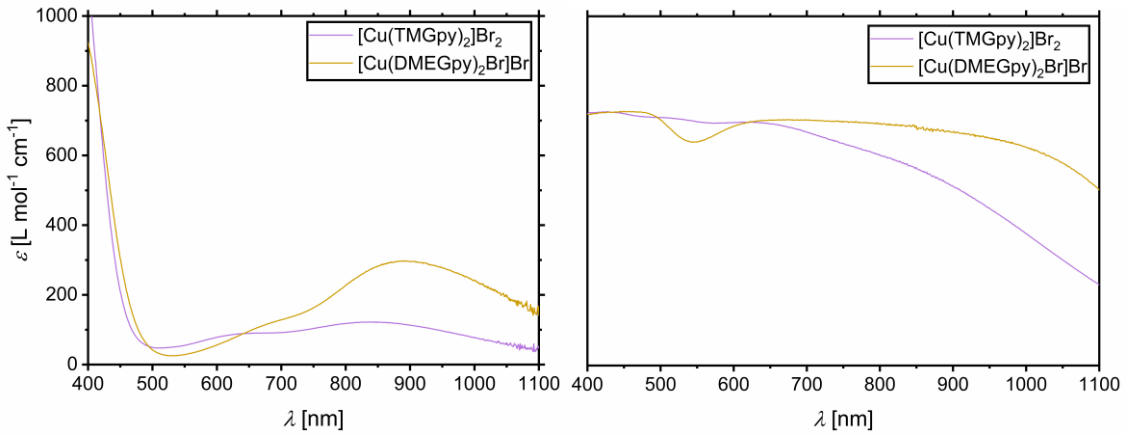


**Fig. S35** UV/Vis spectra of 2.5 mM **C5** and **C6** complex solutions in MeCN (left) and in the solid state (right).

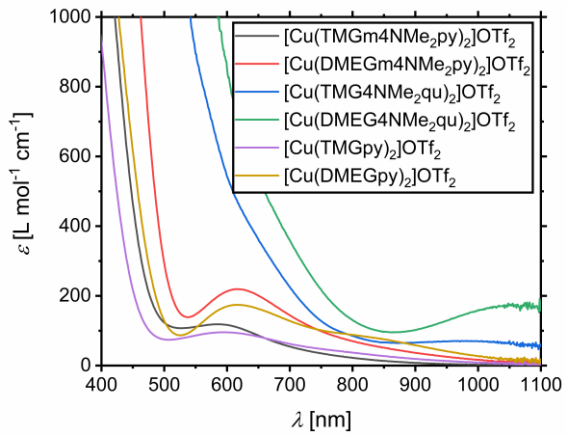


**Fig. S36** UV/Vis spectra of various 2.5 mM complex solutions in MeCN.

## EPR-spectra

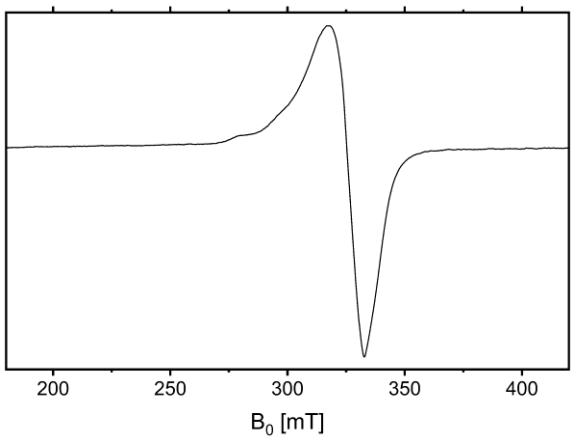


**Fig. S37** Experimental X-band EPR spectra of frozen 5 mM **C2** complex solution in MeCN at 77 K.

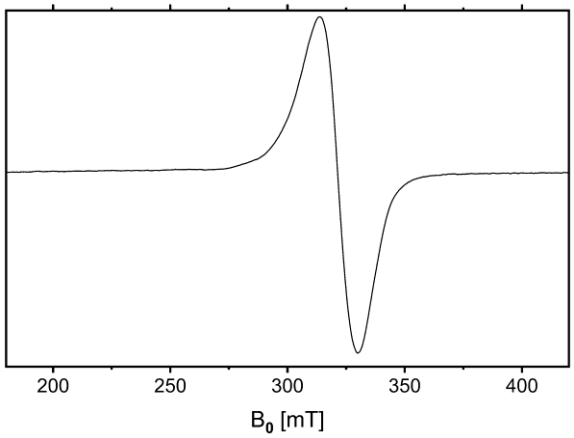


**Fig. S38** Experimental X-band EPR spectra of frozen 5 mM **C3** complex solution in MeCN at 77 K.

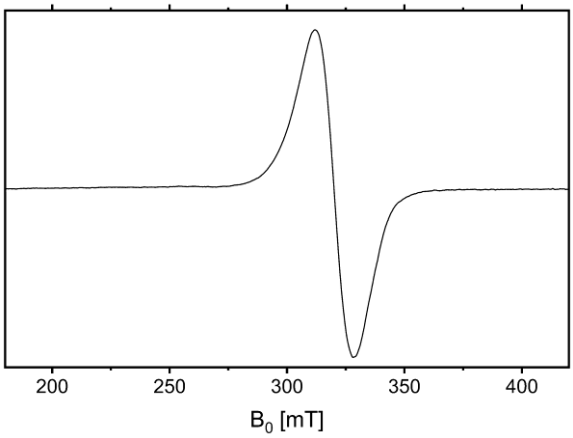


**Fig. S39** Experimental X-band EPR spectra of frozen 5 mM **C4** complex solution in MeCN at 77 K.

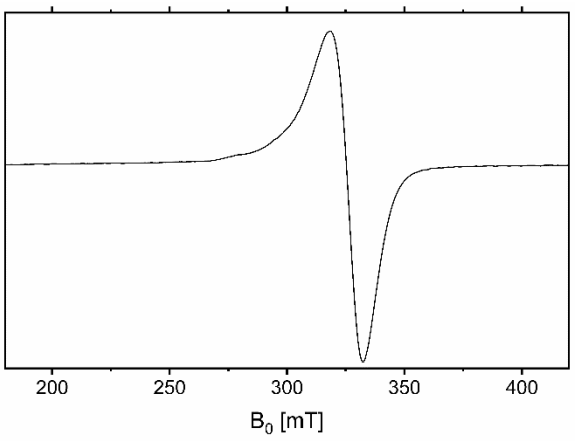


**Fig. S40** Experimental X-band EPR spectra of frozen 5 mM **C5** complex solution in MeCN at 77 K.

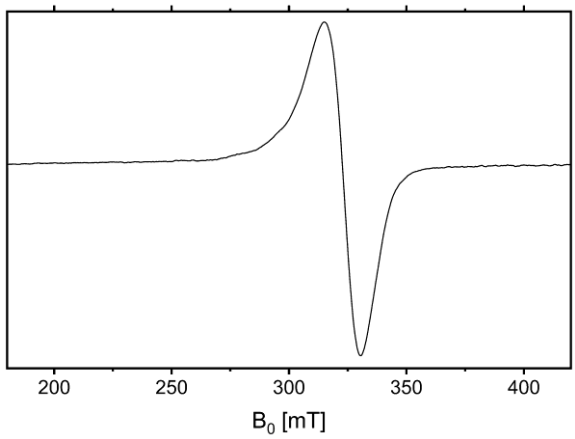


**Fig. S41** Experimental X-band EPR spectra of frozen 5 mM **C6** complex solution in MeCN at 77 K.

**Table S8** Landé g factors and A values of the $CuBr_2$ complexes **C1-B**, **C2**, **C3**, **C4**, **C5** and **C6**.

| | **C1-B** | **C2** | **C3** | **C4** | **C5** | **C6** |
|---|---|---|---|---|---|---|
| $g_1$ | 1.98 | $g_{iso}$ = 2,249 | $g_{iso}$ = 2,249 | $g_{iso}$ = 2,294 | $g_{iso}$ = 2,294 | $g_{iso}$ = 2,241 |
| $g_2$ | 2.06 | | | | | |
| $g_3$ | 2.21 | | | | | |
| $A_1$ [G] | 46 | | | | | |
| $A_2$ [G] | 1 | | | | | |
| $A_3$ [G] | 152 | | | | | |

## Notes and references


1 T. Rösener, O. Bienemann, K. Sigl, N. Schopp, F. Schnitter, U. Flörke, A. Hoffmann, A. Döring, D. Kuckling, S. Herres-Pawlis, *Chem. Eur. J.* **2016**, *22*, 13550-13562.
2 L. Yang, D. R. Powell, R. P. Houser, *Dalton Trans.* **2007**, 955-964.
3 A. W. Addison, T. N. Rao, J. Reedijk, J. van Rijn, G. C. Verschoor, *J. Chem. Soc., Dalton Trans.* **1984**, 1349-1356.
4 V. Raab, K. Harms, J. Sundermeyer, B. Kovačević, Z. B. Maksić, *J. Org. Chem.* **2003**, *68*, 8790-8797.